Icarus 453 (2026) 117048

Contents lists available at ScienceDirect

Icarus

journal homepage: www.elsevier.com/locate/icarus

Research Paper

The dynamical survival of binary near-Earth asteroids: Application to (65803) Didymos, (66391) 1999 KW4, and (101955) Bennu

Rachel H. Cueva [a,*], William F. Bottke [b], Jay W. McMahon [a], David Nesvorný [b], Kevin J. Walsh [b], David Vokrouhlický [c], Harrison F. Agrusa [d]

[a] Smead Department of Aerospace Engineering Sciences, University of Colorado Boulder, 3775 Discovery Dr., Boulder, CO 80303, USA
[b] Solar System Science & Exploration Division, Southwest Research Institute, 1301 Walnut St., Suite 400, Boulder, CO 80302, USA
[c] Institute of Astronomy, Charles University, V Holešovičkách 2, CZ-18000, Prague 8, Czech Republic
[d] Université Côte d'Azur, Observatoire de la Côte d'Azur, CNRS, Laboratoire Lagrange, Nice, France

ARTICLE INFO

Keywords:
Asteroid
Dynamics
Satellites of asteroids
Near-Earth objects
Resonances, orbital
Tides, solid body

ABSTRACT

The steady-state population of asteroids within the near-Earth object (NEO) population is continuously replenished by the migration of asteroids from the main asteroid belt. These bodies are delivered to NEO space through mean motion and secular resonances with the outer planets. Roughly 15% of the NEO and small main belt asteroid populations are estimated to be binary systems. Many small bodies are also "failed binaries," – systems who were at one point mutually bound but are no longer co-orbiting – with some binaries existing as escaped asteroid pairs and ~30% of the population believed to be contact binaries, underscoring the ubiquity of binary formation and the importance of these systems in the broader context of small body evolution. However, it remains unclear whether observed NEO binaries retained their satellites from an initial formation in the main belt, or if these satellites formed later during their lifetime in NEO space. In this study, we present a model to constrain the dynamical survivability of binary asteroids transported from the 3:1 mean motion resonance with Jupiter and the ν_6 secular resonance. Using pre-computed migration pathways from these main belt resonance source regions from the near-Earth object population model, NEOMOD, we simulate the evolution of test binary systems as they migrate into NEO space. Our analysis examines how frequent close encounters with the inner planets and binary orbit evolution through tidal dissipation and the binary Yarkovsky–O'Keefe–Radzievskii–Paddack (BYORP) effect influence the stability and disruption of these systems. We evaluate the evolution of NEO binary systems (66391) 1999 KW4 and (65803) Didymos to determine the likely source regions of their satellites and their expected lifetimes across the inner solar system. We find that 1999 KW4, and by extension other binary NEOs with heliocentric orbits deep into NEO space, are significantly more likely to have formed their satellites in NEO space. We observe Didymos to have a significant probability of having formed its satellite in the main belt, with surviving systems persisting for longer timescales than previously expected due to a strong dependence on tidal-BYORP equilibrium. Additionally, we find that binary mutual orbit inclinations may be produced by close planetary encounters. Finally, we assess the possibility that the single asteroid (101955) Bennu once had a satellite that was lost during its migration from the main belt to explain its top-like shape. We find this scenario to be possible and thus cannot be ruled out as part of Bennu's dynamical history. Together, these results provide new insight into the origins and evolution of binary asteroids.

1. Introduction

Binary asteroids play a crucial role in our understanding of how small rocky bodies physically evolve in response to collisions, non-gravitational forces, and close encounters with planets. Binarity is quite common in the small main belt asteroid (SMBA) and near-Earth object (NEO) populations, with "small" defined as asteroids with diameters less than 10 km (Ćuk and Nesvorný, 2010). Approximately 15% of asteroids in the NEO population and SMBA population for primary diameters less than 15 km in the inner main belt are binaries (Margot et al., 2002; Pravec et al., 2006, 2016; Pravec, 2025) – where two bodies orbit a mutual barycenter – and about 30% are thought to be contact binaries (Virkki et al., 2022) — a bilobate shape which

* Corresponding author.
E-mail address: Rachel.Cueva@colorado.edu (R.H. Cueva).

https://doi.org/10.1016/j.icarus.2026.117048
Received 14 January 2026; Received in revised form 1 March 2026; Accepted 12 March 2026
Available online 18 March 2026

could plausibly be an end case of a former orbiting system whose two components have since collided with each other (note that this is not the only mechanism to form contact binaries). An example of the latter is the asteroid Itokawa and its two distinct lobes imaged by JAXA's Hayabusa mission (Kawaguchi et al., 2008). Additionally, most of these small bodies are suspected to be rubble piles, which are loose conglomerates of rock fragments held together by their own weak self-gravity (Walsh, 2018; Jacobson and Scheeres, 2011a). This structure has been supported by several up close observations of the rocky surfaces of single and binary asteroids, such as Bennu via NASA's OSIRIS-REx mission (Lauretta et al., 2017), Ryugu through JAXA's Hayabusa2 mission (Watanabe et al., 2017), Didymos and its satellite Dimorphos through the NASA DART impact (Daly et al., 2023; Chabot et al., 2024), and Dinkinesh and its satellite Selam from the Lucy spacecraft's flyby of the system (Levison et al., 2024). In the case of Dinkinesh, the existence of Selam was completely unknown until it was discovered by the Lucy spacecraft. Moreover, Selam was also the first ever observed contact binary satellite; this multi-layered binarity further attests to the prevalence of these types of systems.

While binary systems are widespread throughout the present day SMBA and NEO ($q_h < 1.3$ AU, $Q_h > 0.983$ AU) populations, there are many avenues through which the system can be eliminated, such as collisional disruption by an external body or between the two binary components themselves. Such events often occur as a byproduct of a binary asteroid's evolutionary lifecycle (Ćuk, 2007; Ćuk and Nesvorný, 2010). To avoid confusion, it is useful to define the possible histories for a binary asteroid.

A binary asteroid consists of two components: a primary and a secondary. Here we assume that the primary is a factor of three to five times larger than the secondary, which is true for most SMBAs and NEOs; observations suggest binaries with equal size components are rare among these populations (Ćuk and Nesvorný, 2010). A few asteroids are also known to have multiple moons (Margot et al., 2015; Jacobson and Scheeres, 2011a; Fang and Margot, 2011b), but for the sake of simplicity, we will fold these unusual systems into the term binary asteroid.

The secondaries of SMBA and NEO binaries can form through one of several mechanisms: (i) a sub-catastrophic collision where ejected material remains gravitationally bound to the original body and re-accumulates into a satellite (Weidenschilling et al., 1989; Durda et al., 2004); (ii) a collision with a larger body that ejects fragments that become the primary and secondary in a bound mutual orbit while escaping the largest remnant of the collision (Durda et al., 2004, 2007); (iii) tidal disruption during a close encounter with a planet (Walsh and Richardson, 2006, 2008); or (iv) the primary spinning so rapidly – due to processes such as YORP spin-up or volatile loss – that it sheds mass, with the resulting fragments coalescing to form a gravitationally bound secondary (Walsh et al., 2008; Jacobson et al., 2016; Agrusa et al., 2024).

A SMBA primary has two common end states. It can continue existing in the main belt until it undergoes an impact that causes a catastrophic collision, or it can reach a main belt resonance that could potentially propel it into the planet-crossing region. In the latter case, it transitions into a NEO primary (Bottke et al., 2002).

A NEO primary can experience several possible end states. The most common outcomes involve a collision with the Sun, an impact with one of the terrestrial planets, or ejection from the inner solar system following a close encounter with Jupiter. Less frequently, the primary may be catastrophically disrupted by a collision or may approach the Sun closely enough to undergo thermal disintegration. The dynamical timescale to reach any of these end states typically ranges from a few million years (Myr) to a few tens of millions of years (Gladman et al., 2000; Bottke et al., 2002; Nesvorný et al., 2023).

With these end states in mind, we can now consider what happens to a given SBMA or NEO binary. It is often hypothesized that both may experience multiple episodes of satellite formation and destruction until they reach an end state.

There are several ways to destroy a binary asteroid. Small rubble piles are affected by secular perturbations caused by mutual gravitational tides and re-emission of absorbed solar radiation (Ćuk and Burns, 2005; Goldreich and Sari, 2009; McMahon and Scheeres, 2010b; Jacobson and Scheeres, 2011a). These effects may cause the secondary to collide with the primary or escape the system. For NEOs, the timescales for such actions are 10^5 years (Ćuk, 2007). A secondary can also be disrupted by a collision, with the timescale dependent on the primary's orbit and the size of the secondary (Bottke et al., 2025). As NEO binaries evolve within the planet-crossing zone, they can also undergo close encounters with the terrestrial planets – most frequently with Earth and Venus – that can potentially disrupt or strip the satellite from the primary body (Walsh and Richardson, 2008; Fang and Margot, 2011a; Bottke et al., 2025).

Additional satellites may form around the primary, either before or after the loss of the initial secondary. Over time, this can result in the development of typical binary systems with a single-component, multi-component satellites, or even triple asteroid systems (Jacobson and Scheeres, 2011a; Fang and Margot, 2011b). It is also possible that the new moon gravitationally interacts with an existing moon. Such events may cause a merger, as was likely the case for Selam (Raducan et al., 2025), or it could destroy the binary, with one satellite escaping while the another crashes back into the primary. The latter mechanism might be a possible way to create asteroid pairs, where the two bodies have fully split from a bound mutual orbit but follow very similar heliocentric paths (Vokrouhlický and Nesvorný, 2008; Pravec et al., 2010; Jacobson and Scheeres, 2011a; Pravec et al., 2019). Failed binaries may also manifest themselves as starving asteroid families (such as the case of Lucascavin family; Vokrouhlický et al., 2024).

Ultimately, many NEOs are binaries, but there is a lack of knowledge surrounding the source regions of the satellites (Margot et al., 2002; Walsh and Richardson, 2008). Can NEO binaries form and keep a secondary all the way back from the main belt, or are the satellites mainly forming within the NEO region? This study integrates the current understanding of various aspects of near-Earth and main belt binary asteroid evolution into a unified model. The overarching goal is to glean deeper insights into the dynamical survivability of binary asteroids during migration (i.e., specifically, the conditions under which an asteroid can retain its satellite) and to determine their dynamical lifetimes throughout the inner solar system.

The primary contribution of this work is the development of a binary survivability model that integrates key aspects of binary asteroid evolution. Our model builds on many previous studies which have already investigated the individual components in considerable detail. Section 2 summarizes the individual parts that go into our model. Section 3 describes the approach to our model, including migration simulations and chosen asteroid systems of interest. Section 4 presents the key results from the model and Section 5 discusses implications of the results. We summarize and conclude in Section 6.

2. Background

2.1. Typical characteristics of binary NEOs and SMBAs

Before delving into the details of how a binary system can be disrupted, it is important to first establish the observed link between binary NEOs and SMBAs. There are a few shared characteristics among these groups that provide clues about their initial formation and subsequent evolution. These properties typically consist of a larger primary body <10 km in diameter and a smaller secondary body on the order of 20%–40% of the primary's size (Pravec et al., 2016). The systems tend to have a physically circular, tight mutual orbit in the plane of the primary's equator ($\sim 2R_p \leq a \leq 8R_p$ where R_p is primary radii; Pravec et al., 2006; Jacobson et al., 2013) and an oblate spheroid

shaped, rapidly-rotating primary asteroid near its rotational break-up limit (with the typical spin period ranging from 2.2 to 3.6 h; Pravec et al., 2006; Pravec, 2025). (Note these values are based on the binary asteroid parameters database, last updated in 2019; Pravec et al., 2019). The secondaries are often ellipsoidal in shape with elongation ratios on the order of $a/b \lesssim 1.5$ (where $a > b > c$ are the semi-axes of an ellipsoid; Pravec et al., 2016). The spin poles of the two bodies tend to be aligned with the mutual orbit plane.

The similar distribution of binary systems in both the NEO and main belt regions suggests a shared mechanism responsible for the formation of these small binaries (Pravec and Harris, 2007; Walsh et al., 2008). The likely mechanism making binary asteroids within this size range is mass shedding caused by YORP-induced spin-up. The YORP effect is the torque resulting from the thermal re-radiation of absorbed solar radiation pressure (SRP) acting on an asteroid. Due to asymmetries in shape, this re-emission is not constant over time and causes a net torque on the asteroid, either increasing or decreasing its spin rate (Rubincam, 2000; Bottke et al., 2006; Vokrouhlický et al., 2015). If the asteroid is spun up beyond its critical disruption limit, material may be shed from its equator. From there, the ejecta may crash back into the primary or re-accumulate in orbit to form a secondary satellite. Walsh et al. (2008), Agrusa et al. (2024).

The precise nature of the YORP spin-up formation mechanism remains a topic of debate in the literature. Possibilities range from the gradual accretion of ejected material (Walsh et al., 2008; Agrusa et al., 2024) to landslide events (Scheeres, 2015; Agrusa et al., 2022) to the detachment of a single fragment from the primary (Scheeres, 2007b). Despite this, YORP spin-up is considered the most probable driver of small binary asteroid formation because it can account for the observed shared properties of NEO and SMBA binary asteroids. The challenge lies in determining whether we can distinguish between binary systems that were successfully injected into the NEO region without losing their satellites and those that were formed in situ within the NEO population. Identifying differences between the two scenarios would have major implications for understanding the ages, tidal evolution timescales, and material strengths of these bodies.

For example, if some NEO binaries originated in and survived migration from the main belt, their ages could potentially be tied to longer collisional lifetimes, rather than their dynamical end state ages of a few Myr to a few tens of Myr within NEO space (Taylor and Margot, 2011).

2.2. Tidal-BYORP dynamical evolution

There are two main secular perturbations that drive binary asteroids down different evolutionary pathways: re-emission of solar radiation and mutual body tides. Over time, these pathways can lead to escape of the satellite or collision of the two asteroids. The first effect is called binary YORP or "BYORP". Similar to the YORP effect on a single asteroid, solar radiation can also affect binary systems as the satellite acts as an asymmetric appendage to the primary (Ćuk and Burns, 2005). Asymmetries in the secondary's shape leads to a net torque on the system driven by uneven thermal re-emission of absorbed solar radiation, which can expand or shrink the mutual orbit depending on the exact geometry of the secondary.

The BYORP effect is further complicated by the complex gravitational environment of small binary asteroids. These systems exhibit highly non-Keplerian dynamics due to the strong coupling between their orbital and rotational motions (Scheeres, 2006). Typically these systems are dynamically relaxed, or "singly-synchronous", which means the satellite's spin period equals the mutual period with the same side of the satellite always facing the primary. The secondary can also experience "librations", which are bounded oscillations about the singly-synchronous equilibrium.

Near-synchronous rotation is a key requirement of the BYORP effect (McMahon and Scheeres, 2010b). As shape asymmetries cause uneven thermal re-radiation, synchronous rotation ensures a consistent geometry between the satellite's leading and trailing hemispheres. This stability allows the uneven net force to accumulate over time, typically on timescales of tens to hundreds of thousands of years. It gradually drives secular changes in the secondary's orbit (Ćuk and Nesvorný, 2010), even in the presence of small librations.

In a situation where the libration oscillations become unbounded, however, the secondary's moments of inertia and mutual orbit eccentricity can cause the secondary to either tumble or roll about its long axis (commonly referred to as the "barrel roll" configuration; Ćuk et al., 2021). This means there will no longer be a fixed leading and trailing hemisphere. As a result, the re-emission of solar radiation becomes random and will not accumulate over time in a secular manner. This effectively "turns off" the BYORP effect, rendering it incapable of influencing the orbital dynamics.

The state-of-the-art BYORP model was developed by McMahon and Scheeres (2010b,a), which implements the theory from Scheeres (2007a). In summary, the method represents SRP as a Fourier series that is periodic with respect to the secondary's rotation. Given a faceted shape model for the secondary, a set of Fourier coefficients are computed up to a specified order, n. The coefficients and SRP expressions can then be incorporated into a set of equations of motion and numerically propagated to assess dynamical evolution due to BYORP.

However, this highest-fidelity method to quantify the BYORP effect is computationally inefficient. Therefore, we rely on a simplified first-order analytical model for our work. In this BYORP representation, we use only the dominant Fourier coefficient, referred to simply as the "BYORP coefficient", or B. This dimensionless coefficient correlates to the along-track motion of the mutual orbit. A positive B corresponds to orbit expansion, while a negative B corresponds to orbit contraction. The typical estimated value of B is on the order of 10^{-3}–10^{-2}. This single coefficient is numerically computed along with the full set of Fourier coefficients using the methods in Scheeres (2007a) and McMahon and Scheeres (2010a), since BYORP has yet to be measured on an actual body. The typical values are derived from known faceted satellite shape models and are a function of the satellite's reflective properties and the solar latitude. More pronounced shape asymmetries result in a higher magnitude, which in turn leads to a stronger effect and a quicker rate of dynamical evolution.

To first order, the evolution of the orbital semimajor axis and eccentricity is computed using the following equations:

$$\dot{a}_B = \pm \frac{3 H_\odot B}{2\pi} \left(\frac{a^{3/2}}{\omega_d \rho R_p^2} \right) \frac{\sqrt{1+q_0}}{q_0^{1/3}} \tag{1}$$

$$\dot{e}_B = \mp \frac{3 H_\odot B}{8\pi} \left(\frac{a^{1/2} e}{\omega_d \rho R_p^2} \right) \frac{\sqrt{1+q_0}}{q_0^{1/3}} \tag{2}$$

where a and e are the semimajor axis in terms of primary radii (R_p) and eccentricity of the binary mutual orbit, respectively, ρ is the bulk density of the binary system, and q_0 is the mass ratio between the secondary and primary (Jacobson and Scheeres, 2011b). The quantity $\omega_d = \sqrt{4\pi G \rho / 3}$ is the surface disruption spin limit for a sphere (with G being the gravitational constant) (Murray and Dermott, 1999). The quantity $H_\odot$ is defined as:

$$H_\odot = \frac{F_\odot}{a_\odot^2 \sqrt{1-e_\odot^2}} \tag{3}$$

with $F_\odot = 1 \times 10^{14}$ kg km s^{-2} being the solar radiation constant, and $a_\odot$ and $e_\odot$ being the binary's current heliocentric semimajor axis and eccentricity, respectively (McMahon and Scheeres, 2010b,a).

In addition to the BYORP effect, the orbit and rotational dynamics of the binary system are also affected by mutual body tides. This dissipative effect arises from gravity gradients reciprocally imparted on the primary and secondary bodies. It is important to note that the exact mechanism and strength by which tides act on a binary remain

poorly understood and are the subject of significant debate in the literature. However, there is general agreement that tides raised on the secondary work to synchronize its rotation. This is typically the fastest tidal process and can dampen librations over timescales ranging from 100 to 1000 years (Goldreich and Sari, 2009; Meyer et al., 2023b; Cueva et al., 2024).

Tides are ultimately working to synchronize both the secondary and the primary and reach the doubly-synchronous tidal end state (Jacobson and Scheeres, 2011b). Given that the primaries in these systems are typically rapid rotators, their synchronization timescales can be substantially longer than 100 to 1000 years. Consequently, as the primary undergoes spin-down, angular momentum is transferred into the mutual orbit, resulting in a gradual secular expansion of the orbit.

The strength of tides is dependent on the internal structure of these bodies, and we adopt the k_2/Q strength model. This is a ratio of the degree of tidal deformation (k_2) to the efficiency of tidal energy dissipation (Q), and assumes a constant tidal frequency and friction-induced nonelastic tidal deformation (Goldreich and Sari, 2009; Nimmo and Matsuyama, 2019). While we recognize alternative tidal dissipation theories, such as viscosity-driven approaches (Efroimsky, 2015) or hypothetical short-lived episodes of high dissipation rather than gradual dissipation (Ćuk et al., 2024), we choose to stick with the friction-based k_2/Q representation due to its relative simplicity and frequent use throughout the literature (Jacobson and Scheeres, 2011b; Meyer et al., 2023b; Cueva et al., 2024).

Once again, we use a first-order analytical representation of tidal evolution, where the change in semimajor axis and eccentricity are:

$$\dot{a}_T = 3\frac{k_p}{Q}\left(\frac{\omega_d}{a^{11/2}}\right) q_0\sqrt{1+q_0} \tag{4}$$

$$\dot{e}_T = \frac{57k_p q^{1/3} - 84k_s}{8Q}\left(\frac{\omega_d e}{a^{13/2}}\right) q_0^{2/3}\sqrt{1+q_0} \tag{5}$$

where k_p and k_s are the tidal Love numbers of the primary and secondary, respectively (Jacobson and Scheeres, 2011b; Murray and Dermott, 1999). These evolutionary equations are derived from the tidal torque expressions in Murray and Dermott (1999), where the strength of the torque scales $\propto a^{-6}$. As a result, tidal strength diminishes rapidly as the secondary moves farther from the primary. If the secondary's distance from the primary becomes sufficiently large, tidal-driven orbital expansion slows significantly, and the tides acting on the secondary may become too weak to resynchronize its rotation.

Tides and BYORP do not act independently of each other. Instead, their coupled interactions can give rise to a wide range of evolutionary behaviors. This interplay makes it challenging to fully disentangle the individual contributions of tides and BYORP to the overall observed orbital drift rate. Tides are always expanding the orbit for these systems, but BYORP can shrink or grow the orbit. If B is positive, these expansive systems can lead to wide asynchronous binaries, where the large semimajor axis weakens tides significantly and destabilizes the secondary (Jacobson et al., 2013), or asteroid pairs, where the two bodies have escaped their bound mutual orbit and are on similar heliocentric orbits (Pravec et al., 2010; Jacobson and Scheeres, 2011a). Thus, it is possible that a main belt binary system could lose a satellite from expansive BYORP and tides to create an asteroid pair, preventing it from fully becoming an NEO binary.

Systems with contractive BYORP can lead to contact binary systems, or induce a theoretical tidal-BYORP equilibrium where the torques of contractive BYORP and expansive tides cancel out (Jacobson and Scheeres, 2011b). It has been hypothesized that this equilibrium configuration can be long-term stable compared to the other tidal-BYORP evolutionary pathways. Recent work in Wang and Hou (2021) suggests that a system may exist in this equilibrium state for timescales of $>10^6$ years. They could potentially remain in this state indefinitely unless adequately perturbed by an external collision or planetary encounter (Jacobson et al., 2016).

The analytical equation for the location of this equilibrium semimajor axis (a^*) is derived from Eqs. (1) and (4), and is expressed as:

$$a^* = \left(\frac{2\pi k_p \omega_d^2 \rho R_p^2 q_0^{4/3}}{BH_\odot Q}\right)^{1/7} \tag{6}$$

This theoretical equilibrium semimajor axis has been numerically demonstrated to be stable in the presence of additional dynamics other than BYORP and primary tides (Cueva et al., 2024). This mechanism could even play a key role in enabling the long-term survivability of binary NEOs and SMBAs.

2.3. Planetary encounters

The effects of planetary encounters on binary asteroids has been studied extensively throughout the literature. Original analytical expressions for the change in a binary asteroid system's orbital energy – and consequently, semimajor axis – due to a planetary flyby were derived by Farinella (1992), Farinella and Chauvineau (1993) and Chauvineua et al. (1995). Eccentricity change of a binary star system due to an encounter with a third star was derived by Heggie and Rasio (1996), and both eccentricity and inclination changes due to an unbound perturber was evaluated by Collins and Sari (2008), with specific applications to Kuiper Belt binaries.

Numerical models have investigated the feasibility of planetary encounters as a source of binary asteroids. Walsh and Richardson (2006) performed N-body simulations to study the tidal disruption of a progenitor body and potential formation of a satellite by an Earth encounter. Bottke and Melosh (1996) looked at the formation of co-orbiting binary fragments from tidal break-up of rubble piles and contact binaries as an explanation of the fraction and properties of doublet craters observed on the inner planets. Fang and Margot (2011a) numerically studied how a binary mutual orbit between the primary asteroid and its satellite can change in shape and orientation following an Earth flyby, analyzing a wide range of encounter geometries and comparing to analytical approximations. Araujo and Winter (2014) analyzed the stability of binary NEOs as they undergo Earth encounters and transition between different near-Earth dynamical classes (e.g., Amor, Apollo, and Aten).

The highest fidelity numerical model of the effect of planetary encounters on binary asteroid dynamics was developed by Meyer and Scheeres (2021) and implemented into the General Use Binary Asteroid Simulator (GUBAS) (Davis and Scheeres, 2020). This model builds off of the foundation in Fang and Margot (2011a), where the flyby is modeled as an impulsive perturbation with all spherical components. However, unlike in Fang and Margot (2011a) and other past studies, Meyer and Scheeres (2021) accounts for the coupled orbital and rotational dynamics in these non-Keplerian systems by allowing for non-spherical asteroid shapes. This allows for analysis on what combinations of flyby parameters trigger the secondary's tumbling state, in addition to what parameters lead to complete disruption of the system (i.e., stripping of the satellite or collision with the primary). The tumbling state is important for modeling BYORP evolution following a flyby since this configuration renders BYORP inactive. Additionally, while the effects of the flyby on the binary orbit behave as impulsive, GUBAS includes the perturbing planet in simulations to include its gravity at each time step.

The largest complication with the GUBAS code is computation time, with a single flyby taking on the order of ~15–30 s to simulate. This quickly compounds and becomes significant when analyzing hundreds of successive flybys per each test binary system across tens to hundreds of transportation routes from main belt to NEO space. Because of this, our model utilizes the analytical equations in Fang and Margot (2011a) and will be summarized here.

To first-order, the change in the mutual orbit semimajor axis, eccentricity, and inclination due to a planetary encounter can be described as:

$$\Delta a \approx 1.48\sqrt{\frac{G}{M}}\frac{M_{pl}a^{5/2}}{v_\infty q^2} \tag{7}$$

$$\Delta e \approx 1.89\sqrt{\frac{G}{M}}\frac{M_{pl}a^{3/2}}{v_\infty q^2} \tag{8}$$

$$\Delta i \approx 0.75\sqrt{\frac{G}{M}}\frac{M_{pl}a^{3/2}}{v_\infty q^2} \tag{9}$$

where G is the gravitational constant, M is the total mass of the binary system, M_{pl} is the planetary mass, a is the Keplerian semimajor axis of the mutual orbit, v_∞ is the hyperbolic excess speed of the flyby, and q is the close approach distance of the flyby. These equations represent the average change in these values over all encounter geometries, with the constants in the equations arising from this averaging process (Fang and Margot, 2011a; Collins and Sari, 2008).

A detailed comparison of these analytical approximations against the results of the full numerical GUBAS simulations was performed by Meyer and Scheeres (2021). They found that while the two approaches generally agree to within one order of magnitude, the analytic equations tend to over-estimate the change in each element. This is likely due to the discrepancy in using Keplerian orbit elements to describe non-Keplerian systems like binary asteroids (Meyer et al., 2023a), since the orbital and rotational dynamics for these systems are highly coupled. However, since this study represents the first known attempt to model the overall survivability of binary asteroids through multiple distinct mechanisms, an order-of-magnitude approximation is deemed a sufficient starting point to make this initial large scale survivability study computationally tractable. We note that survivability probabilities are expected to decrease if the analytical approximations deviate too far from the full numerical simulations.

A limitation of using purely analytical expressions is the absence of the effects on the satellite's rotational motion. In order to account for this, we look at the flyby parameter for a given encounter. This single coefficient represents the overall impact of the flyby by linking the incoming binary's orbital size and mass, the mass of the encountering planet, and the flyby's distance and speed. It is defined as:

$$P = \sqrt{\frac{G}{M}}\frac{M_{pl}a^{3/2}}{v_\infty q^2} \tag{10}$$

This value can be used as a proxy for when, on average, we can qualitatively expect the satellite to start tumbling. Based on a series of GUBAS simulations for a system similar to 1999 KW4, this cut-off value for tumbling was determined to be approximately 0.1. Since the flyby parameter changes primarily with encounter distance, flyby speed, or the binary mutual orbit semimajor axis entering into the flyby, this means that any combination of those three variables resulting in a flyby parameter greater than 0.1 will trigger tumbling. This result is further supported by Fig. 11 in Meyer and Scheeres (2021), which conducted a similar study for a generic representative NEO binary.

The flyby parameter can also be used to assess when, on average, we should expect the satellite to either be stripped from or collide with the primary. Eqs. (7)–(9) do not always capture these outcomes as simple checks based on the Hill sphere radius, tidal disruption radius, or Roche limit of the asteroid do not account for the effects of encounter speeds. Thus, the flyby parameter was used to better match numerical outcomes from GUBAS. Using the same approach as the cutoff for tumbling behavior, we found that systems tend to be numerically disrupted from the flyby at $P \approx 0.2$.

To visualize how this parameter relates to dynamical behavior, we will use near-Earth binary asteroid system 1999 KW4 as an example. Fig. 1 shows the distributions of flyby parameters for 300 simulated Earth encounters with GUBAS. Flyby distances ranged from 2 to 30 Earth radii and two v_∞ values of 16 and 24 km/s were used. For a nominal 1999 KW4 system that has a mutual orbit semimajor axis of ~3.9 primary radii (Ostro et al., 2006) heading into a flyby with v_∞ = 16 km/s, planetary encounters with $5.5 \leq q \leq 8$ planetary radii will trigger tumbling and encounters with $q \leq 5.5$ planetary radii will lead to binary disruption, corresponding to our chosen tumbling cut-off ($P = 0.1$) and disruption cut-off ($P = 0.2$). For v_∞ = 24 km/s, this results in tumbling and disruption limits of ~6.4 and ~4.5 planetary radii, respectively.

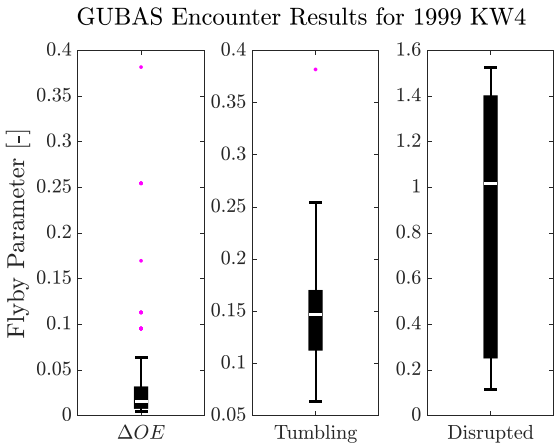

Fig. 1. The distribution of flyby parameters (P) corresponding to simulated Earth encounters for binary asteroid system 1999 KW4 using GUBAS. The left box plot shows cases where the orbit was perturbed and satellite libration was induced, the middle box plot shows cases where satellite tumbling was triggered, and the right box plot shows cases where the binary was fully disrupted (either by escape or collision between the two components). 300 total GUBAS simulations were performed.

From Fig. 1, we can see that while there are some outlier cases, the majority of cases where the binary mutual orbit is perturbed and satellite libration is induced have $P < 0.1$. Likewise, the majority of cases where satellite tumbling was triggered or full disruption occurred fall within $0.1 < P < 0.2$ and $P > 0.2$, respectively, corroborating our selected cut-off values.

The tumbling and disruption P values are used as thresholds within the algorithms described in the following section. These thresholds do not represent strict cut-offs between behaviors, rather where, on average, we can expect qualitative behavior in the binary system to change. Therefore, the cut-offs should be considered as loose thresholds. Refining and fine-tuning these values is left for future work.

3. Methodology

3.1. Migration pathways of asteroids: NEOMOD

Most NEOs originate in the main belt. Kilometer-sized main belt asteroids primarily follow two key transportation routes that increase their eccentricities to the point that they can reach Earth-crossing orbits: (1) the 3:1 mean-motion resonance with Jupiter located at about ~2.5 AU in the main belt, and (2) the ν_6 secular resonance, where an asteroids' heliocentric apsidal precession equals that of Saturn. This resonance is located at the inner edge of the main belt (Minton and Malhotra, 2010). These resonant zones, which are resupplied via the Yarkovsky-induced semimajor axis drift of asteroids and the occasional direct injection of collisional fragments, are responsible for keeping the km-sized NEO population in steady state (Bottke et al., 1994, 2001, 2002, 2006; Morbidelli and Vokrouhlický, 2003; Minton and Malhotra, 2010). These two main resonances are predicted to deliver ~30% of asteroids with absolute magnitude $H \sim 15$ and ~90% of asteroids with $H \sim 28$ in NEO space (Nesvorný et al., 2023, 2024a; Granvik et al., 2016).

The most detailed numerical model simulating the migration pathways of asteroids ejected from resonant zones in the main belt is the near-Earth object model, NEOMOD (Nesvorný et al., 2023, 2024a,b). NEOMOD was constructed by numerically integrating the heliocentric orbits of test asteroids from main belt resonance source regions to NEO space (Nesvorný et al., 2023). Using these results, they constructed residence time probability distributions which provide a map of where NEOs from a given source are statistically likely to be found. Next, they combined these contribution with models of observational selection effects based on data from the Catalina Sky Survey (CSS). This approach enabled them to compare and calibrate the source contributions against NEO observations recorded by the CSS.

The first version of the model utilized 4510 NEO observations over the time period of 2005–2012 (Nesvorný et al., 2023), while the second version was updated to include ∼14,000 new observations over the time period of 2013–2022 (Nesvorný et al., 2024a). The third version of the code includes data from the Wide-Field Infrared Survey Explorer (WISE) mission to compute the size distribution of NEOs (Nesvorný et al., 2024b).

NEOMOD accounts for 12 resonance sources: the 3:1, 5:2, 7:3, 8:3, 9:4, 11:5, and 2:1 resonances with Jupiter, the ν_6 resonance with Saturn, an "inner-belt" source region to account for various interacting weak resonances, the high-inclination source regions for the Hungaria and Phocaeas asteroid families, and a comet source region. The model propagates 10^5 test asteroids from each source for statistical significance, recording their heliocentric orbits every 1000 years until they collide with a planet or the Sun, or are ejected from the solar system (Nesvorný et al., 2023).

For our initial study, we use pathways solely from the 3:1 and ν_6 resonance source regions, as they are the two most efficient sources for km-sized and smaller asteroids (Bottke et al., 2002). All 10^5 migration pathways for each of the 3:1 and ν_6 sources, along with all corresponding encounters with the inner planets recorded up to a distance of 30 planetary radii, were used in our work (provided by D. Nesvorný). Each encounter has a corresponding encounter pericenter distance with a planet q and planetary encounter velocity v_∞. While it is possible that more distant encounters can perturb very wide binaries, Fang and Margot (2011a) found that encounters within 30 planetary radii capture the most significant orbital changes.

3.2. Dynamical survivability model

Our model consists of a pre-processing block and a Monte Carlo simulation block. The process begins by first choosing an existing binary NEO of interest. After identifying such a system, the pre-processing block sifts through all test asteroid migration pathways from the 3:1 and ν_6 resonance sources for runs that come within a specified tolerance of the existing binary's heliocentric orbit (e.g., Bottke et al., 2015). Each matching run is recorded and all orbit states after the time of match are discarded. The corresponding planetary encounters for each migration pathway are then found and recorded.

These pathway and encounter files are then passed to the main Monte Carlo simulation block. The code flow of this main block is visualized in Figs. 2 and 3 and is summarized as follows. All matching NEOMOD migration pathways and their respective planetary encounters for the chosen existing binary system of interest are loaded, and each migration pathway is individually analyzed on a separate computer core. If there are no planetary encounters (which was extremely rare; only one matching pathway of the three systems analyzed later on had no encounters), N test binary systems are initialized and propagated through a single tidal-BYORP evolution arc until the system either reaches the heliocentric state of the observed binary system or is disrupted. Here, we define disruptions as either stripping the satellite from the binary mutual orbit (which is only possible via expansive BYORP in this instance) or colliding with the primary asteroid.

If there are planetary encounters, the code enters a loop where N test binary systems are initialized at the start of each encounter. For example, if there are 100 planetary encounters experienced along the migration pathway from the main belt to the final NEO state, then there would be 100 sets of N test binaries.

To better illustrate how this loop works, we will walk through the first few iterations. We start at the final heliocentric state of the known binary system of interest and work backwards in time through all encounters. On the first iteration, the initial encounter in this instance is the "most recent" encounter relative to the final heliocentric state of the existing binary. In other words, this encounter is equivalent to the latest encounter in time along the migration pathway. At that point, N test binaries are initialized and the first-order encounter equations are propagated through the initial encounter for each test binary. If the satellite is disrupted during the flyby, the simulation is exited for that test binary. If the satellite survives, it is passed to the first-order tidal-BYORP analytical equations and propagated until it reaches the state of the existing binary, where it is either checked for disruption following the tidal-BYORP arc or marked as a complete run.

The second iteration initializes N test binaries at the start of the second most recent encounter, equivalent to the second latest encounter in forward time relative to the initial location in the main belt. Each test binary is propagated through the encounter equations for the new initial encounter, checked for disruption, propagated through a first tidal-BYORP evolution arc if they survived, and again checked for disruption. This iteration now has two total encounters, so the surviving test binaries are propagated through the next planetary encounter in forward time before reaching the final state of the known binary. The second encounter in this iteration is equivalent to the first and only encounter in the previous iteration. Even though we have already simulated this encounter, we re-simulate flyby dynamics again in the second iteration because the incoming binary geometry for each test asteroid is now different from the fixed binary geometry initialized before the encounter in the previous iteration. For example, the binary semimajor axis for each test system will have increased or decreased varying amounts having already undergone an initial encounter and tidal-BYORP evolution arc. Thus, while the flyby distance and speed remains the same, the binary semimajor axis and, consequently, the flyby parameter defined by Eq. (10) will change from previous evolutionary arcs, altering the probability of satellite tumbling or disruption.

This process repeats for each encounter along the migration pathway for all matching migration pathways: Initialize N binaries at the location of each encounter and propagate through successive planetary encounter and tidal-BYORP dynamics until the satellite is lost or the final state of the known binary is reached.

A visualization of this methodology is depicted in Fig. 4. This approach provides statistics on how far back along its migration history the existing binary could have kept its satellite. We chose $N = 50$ initial test binaries as a compromise between statistical significance and computation expediency.

Test binary systems are initialized with a prescribed mutual orbit description (semimajor axis, eccentricity, and inclination relative to the primary's equatorial plane), physical parameters of the primary and secondary bodies (mass and radius for each component assuming spherical shapes and a uniform system bulk density), a qualitative attitude representation, and randomized B and k/Q values. We assume that the satellite is confined to two attitude options: fully dynamically relaxed (i.e., singly synchronous) or fully tumbling (unbounded oscillations), but every system starts as synchronous. Bounded librational motion is ignored for the purposes of this study. For the simulations presented in this work, we use a fixed initial binary semimajor axis, and assume zero mutual orbit eccentricity and inclination with a synchronous secondary.

BYORP values are sampled over magnitudes of 10^{-2} and 10^{-3}, as these represent typical BYORP magnitudes reported in the literature (McMahon and Scheeres, 2010a; Jacobson and Scheeres, 2011b), and are given an equal chance of being positive or negative. Tidal

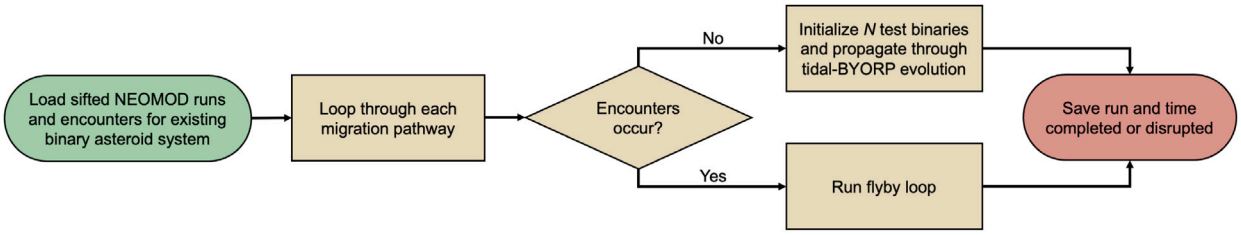

Fig. 2. High level code flow for the main Monte Carlo loop.

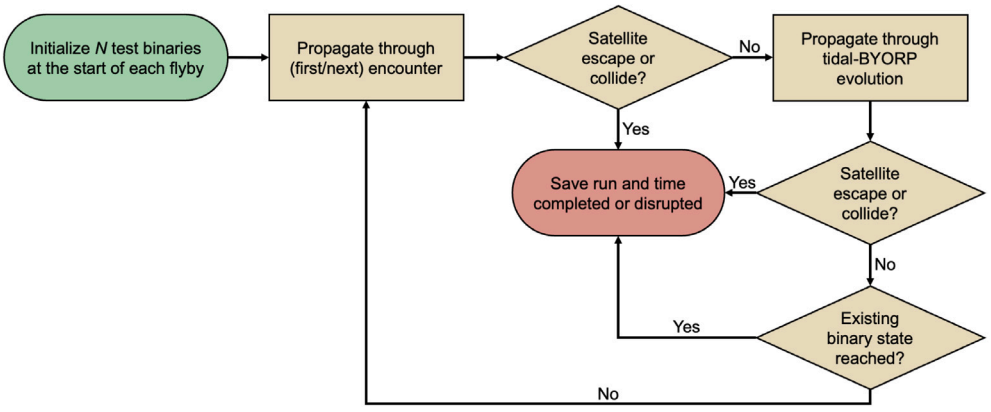

Fig. 3. Iterative planetary encounter loop code flow for the main Monte Carlo loop.

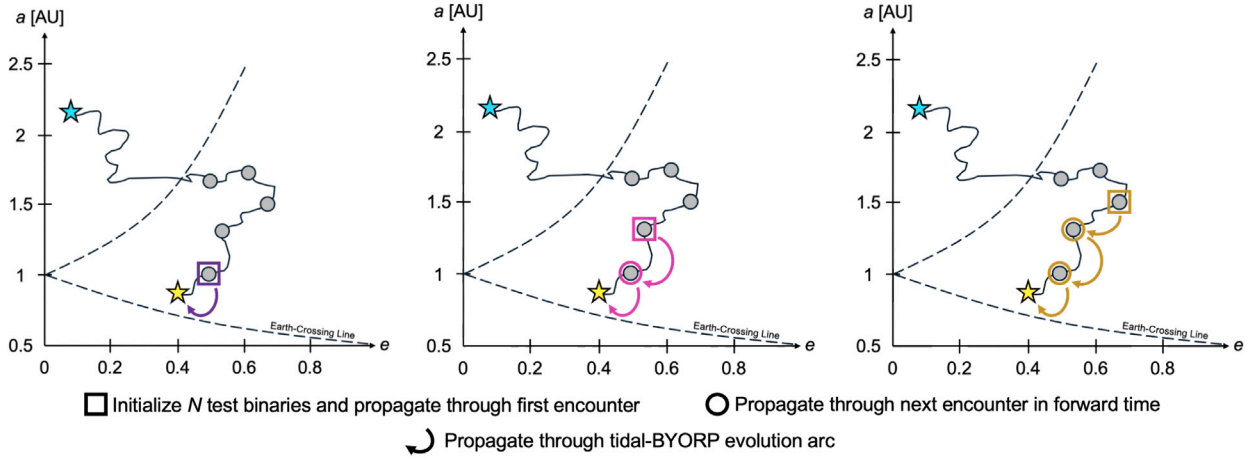

Fig. 4. Visualization of Monte Carlo code flow for the first three iterations of the propagation loop from left to right. The dashed lines indicate the Earth-crossing line that marks the boundary for where encounters with Earth are possible, the solid line is a depiction of a migration pathway starting in the main belt at the location of the cyan star and ending at the location of a known binary system (gold star). The gray circles are locations of planetary encounters. The first iteration (left) initializes N test binaries at the most recent encounter relative to the final heliocentric state, the second at the second most recent encounter (middle), and so on; in each case, binaries are sequentially propagated in forward time through planetary flybys tidal-BYORP evolution arcs until the satellite is disrupted or the present-day binary state is reached.

parameters are sampled over magnitudes 10^{-5} and 10^{-6}. These values were selected based on tidal parameters used in previous modeling efforts (Jacobson and Scheeres, 2011b; Nimmo and Matsuyama, 2019; Meyer et al., 2023b; Cueva et al., 2024). Although the exact tidal strength of rubble piles remains largely uncertain, these estimates are considered adequate given our current state of knowledge. The values for B and k/Q are sampled uniformly over log space and are fixed for the length of the simulation (i.e., we assumed no re-shaping effects during evolution).

The planetary encounters code block in Figs. 2 and 3 is a function that reads in the binary orbit and system parameters, the heliocentric orbit position, and the current flyby information and planet (Mercury, Venus, Earth, or Mars). The magnitude of the change in mutual orbit a, e, and i due to the flyby are computed using Eqs. (7)–(9). These values can either increase or decrease due to a flyby, so each value is given an equal chance of being positive or negative. Perturbations that lead to a non-physical result (e.g., negative eccentricity) are discarded and redrawn. While the first encounter will have N test binaries initialized with all the same geometry and thus the same magnitudes in orbit changes due to the flyby, the signs of the flyby changes are randomly selected. Thus, the test binaries would not evolve identically through the first flyby. Although the choice of initial semimajor axis might affect the resulting behavior from the first encounter, all systems are initialized with starting binary semimajor axes typically expected

as a result from YORP-induced fission satellite formation. Note that orbital parameters with no subscript represent the mutual orbit, while parameters with subscript h distinguish heliocentric values.

The flyby parameter for the current encounter is computed using Eq. (10). If this parameter is greater than 0.1, the satellite is set to tumbling mode. If it is greater than 0.2, the system is marked as destroyed, with the satellite escaping or colliding with the primary depending on the direction of Δa. We also check the Hill sphere and Roche limit of the primary for satellite escape or collision in the event the flyby parameter is less than 0.1. We also perform intermediate checks for eccentricities exceeding one for satellite escape. Recall that the flyby parameter is used in addition to these physical limits to account for the speed of the planetary encounter (e.g., a binary is more likely to be disrupted at slower encounter speeds).

The tidal-BYORP evolution code block processes the updated binary parameters provided by the encounter function and propagates the Eqs. (1), (2), (4), and (5) from the time of the current encounter to the time of either the next encounter or the final state of the known binary. The heliocentric parameters of the test binary are updated every 1000 years due to the cadence at which NEOMOD data is recorded.

The signs of Eqs. (1) and (2) are determined based on the prescribed B for each test binary. If the satellite is tumbling post-flyby, then BYORP is shut off and only the tidal evolution equations are propagated. However, this code block also computes a tidal despinning timescale as a proxy for tidal synchronization by solving for time in the following equation:

$$\frac{1}{\overline{\omega}_s}\frac{d\omega_s}{dt} = \frac{15}{4}\mathrm{sgn}\left(n-\omega_s\right)\frac{k_s}{Q}\left(\frac{\rho_p}{\rho_s}\right)^{3/2}\left(\frac{R_p}{a}\right)^{9/2} n \tag{11}$$

where ω_s is the satellite's spin rate, n is the mean motion of the mutual orbit, and $\overline{\omega}_s = \sqrt{GM_s/R_s^3}$ is the breakup spin rate (with M_s and R_s being the mass and radius of the secondary, respectively) (Goldreich and Sari, 2009). The values ρ_p and ρ_s are the densities of the primary and secondary, respectively; however, this ratio becomes unity since we assume equal densities between the components.

If this timescale is reached prior to the next encounter or the final end state, then the satellite attitude is set to singly synchronous and BYORP evolution is turned back on for the rest of that evolution arc. This block also uses the Hill sphere and Roche limit of the primary to check for satellite escape or collision with the primary, respectively.

We note that while we assume a system bulk density to be consistent with the first-order tidal-BYORP analytical equations outlined in Section 2.2, modest deviations from uniform density between the primary and secondary can modify the tidal despinning timescale by a factor-of-a-few variations. However, these deviations do not tend to change the order of magnitude of the timescales. The despinning timescale is far more sensitive to the mutual orbit semimajor axis, which varies significantly throughout the simulations. Because the tidal damping timescale is compared to the interval between planetary encounters to determine when BYORP evolution resumes, this remains an order-of-magnitude estimate dominated by variations in a rather than non-uniform density.

3.3. Asteroid systems of interest

In order to assess overall survivability of NEO binaries, we have chosen three representative systems to analyze: Didymos and Dimorphos, 1999 KW4 (also commonly referred to as Moshup and Squannit in the literature), and Bennu. The first two are known binaries, while Bennu is a well studied asteroid that possibly had a satellite in the past (Walsh, 2018; Bottke et al., 2025). Their properties are summarized below.

The Didymos system was the target of the NASA DART mission. The spacecraft impacted the satellite Dimorphos in September 2022 (Daly et al., 2023; Chabot et al., 2024). Prior to the up-close images of Dimorphos captured just before impact, the 1999 KW4 system was possibly the most extensively studied and well-characterized binary asteroid system in NEO space (Ostro et al., 2006). Some of the papers discussing the dynamical environment of 1999 KW4 are Scheeres et al. (2006), Fahnestock and Scheeres (2008), McMahon and Scheeres (2010a).

These systems represent typical binary NEOs, exhibiting the characteristics described in Section 2.1. However, each are on very different heliocentric orbits in NEO space. Didymos is an Apollo class NEO ($a_h \geq 1.0$ AU, $q_h \leq 1.0167$ AU), while 1999 KW4 is an Aten class NEO ($a_h < 1.0$ AU, $Q_h \geq 0.983$ AU) (Bottke et al., 2002). Both are Earth-crossing asteroids, meaning they will experience encounters with Earth, but 1999 KW4 has traveled much deeper into NEO space compared to Didymos. Combined with the fact that Atens have Earth-crossing orbits near aphelion, the slowest segment of their orbital trajectory (Michel et al., 2000), this substantially increases the probability of Earth encounters during their dynamical evolution (Araujo and Winter, 2014). Thus, these two binary systems should provide a useful comparison between their respective migration pathways and subsequent evolution.

Bennu was the target of the OSIRIS-REx sample return mission. It successfully collected surface material in 2020, with the samples delivered to Earth on September 2023. The combination of in situ reconnaissance of Bennu with laboratory analysis of its materials have provided us with key insights into the composition, structure, and evolutionary history of primitive, carbonaceous chondrite-like rubble-pile asteroids (Lauretta et al., 2024).

While Bennu does not currently have a satellite, it may have had one in the recent past (Walsh, 2018; Bottke et al., 2025). It was chosen as a case study to assess the likelihood that it once formed a satellite and lost it during its migration through NEO space. Bennu has a relatively rapid spin rate, with a rotational period of 4.3 h, and features a distinct top-shaped structure with a prominent equatorial ridge. Both are characteristics of a primary body in a binary system formed through YORP-induced spin-up (Bottke et al., 2015).

We will investigate the probability of Bennu losing a satellite from planetary encounters and/or tidal-BYORP evolution. The physical and dynamical properties of the three asteroid systems of interest are provided in Table 1 for comparison. Note that Didymos values are those pre-DART impact when the system was suspected to be in a relaxed singly synchronous configuration (Richardson et al., 2022, 2024).

We note that while the ν_6 and 3:1 resonance are the dominant pathways for NEOs in general (Bottke et al., 2002), their relevance can change for individual asteroids. Previous modeling efforts demonstrate that the ν_6 resonance is the most likely source region for Bennu (with a predicted ~82% probability; Bottke et al., 2015). Didymos is suggested to have a >82% probability of coming from the ν_6 resonance source and a ~7% chance of coming form the 3:1 mean-motion resonance (Richardson et al., 2016). Overall statistical models of the NEO population indicate that for asteroids with absolute magnitudes similar to Didymos ($H \sim 18.1$) and 1999 KW4 ($H \sim 16.6$), the ν_6 and 3:1 resonances are the two sources that statistically dominate delivery over all other individual resonance sources (Nesvorný et al., 2023, 2024a; Granvik et al., 2016). This provides further justification for solely analyzing the ν_6 and 3:1 resonance sources for the three selected asteroids.

4. Results

4.1. Dynamical survivability simulations

We simulate the dynamical survivability of Didymos, 1999 KW4, and Bennu using the tool outlined in Section 3.2. Systems are initialized as dynamically relaxed (i.e., circular mutual orbits in the primary's equatorial plane and singly synchronous attitude configurations). Bennu was prescribed a pseudo-satellite modeled off typical NEO satellite parameters. Specifically, we use a mutual orbit separation of $4R_p$ and component size and mass ratios equivalent to those of 1999 KW4.

Each test binary was randomly assigned a B and k/Q value and initialized using the orbital and physical parameters provided in Table

Table 1
Relevant physical and dynamical parameters of chosen NEO systems.

Parameter	Didymos Value	1999 KW4 Value	Bennu Value
Physical System[a]	...	...	...
System Mass	5.3×10^{11} kg	2.488×10^{12} kg	7.329×10^{10} kg
Volume-Equivalent Diameter of Primary	0.730 km	1.317 km	0.490 km
Bulk Density of Primary	2790 kg m^{-3}	1970 kg m^{-3}	1190 kg m^{-3}
Mass of Primary	–	2.353×10^{12} kg	7.329×10^{10} kg
Rotation Period of Primary	2.26 h	2.76 h	4.30 h
Volume-Equivalent Diameter of Secondary	0.150 km	0.451 km	–
Bulk Density of Secondary	2400 kg m^{-3}	2810 kg m^{-3}	–
Mass of Secondary	–	1.350×10^{11} kg	–
Rotation Period of Secondary	11.92 h	17.42 h (assumed)	–
Mutual Orbit[b]	...	...	...
Orbital Separation	1.189 km ($\sim 3.3 R_p$)	2.548 km ($\sim 3.9 R_p$)	–
Eccentricity	<0.03	0.0004	–
Inclination relative to primary's equatorial plane	0 (assumed)	3.2°	–
Mutual Orbit Period	11.92 h	17.42 h	–
Heliocentric Orbit[c]	...	...	...
Family Types	Apollo	Aten	Apollo
Semimajor Axis	1.643 au	0.642 au	1.126 au
Eccentricity	0.383	0.688	0.204
Inclination	3.414°	38.891°	6.035°

[a] Didymos values from Richardson et al. (2024). Note that recent work may suggest a lower Dimorphos density of 1540 kg m^{-3} (Chesley et al., 2025). This would alter the mass ratio of the Didymos system and slightly affect tidal-BYORP evolution, but the mass ratio would overall remain within in the same order-of-magnitude estimate. 1999 KW4 value from Ostro et al. (2006). Bennu primary volume-equivalent diameter and rotation period from Lauretta et al. (2019), primary bulk density and mass from Scheeres et al. (2019).
[b] Didymos values from Richardson et al. (2024). 1999 KW4 orbital separation and eccentricity values from Ostro et al. (2006), inclination value from Scheeres et al. (2006).
[c] Didymos values from the JPL Solar System Dynamics Horizons System (Solution 205 for Epoch 2459957.0 = 2023 Jan 12.5 TDB). 1999 KW4 values from Fahnestock and Scheeres (2008). Bennu values from the JPL Solar System Dynamics Horizons System (Solution 118 for Epoch 2455562.5 = 2011 Jan 01.0 TDB).

Table 2
Initial conditions and parameters for simulations of chosen NEO systems.

Parameter	Didymos Value	1999 KW4 Value	Bennu Value
Physical System	...	...	...
System Bulk Density	2790 kg m^{-3}	2000 kg m^{-3}	1190 kg m^{-3}
Volume-Equivalent Diameter of Primary	0.730 km	1.317 km	0.490 km
Mass of Primary	5.255×10^{11} kg	2.353×10^{12} kg	7.329×10^{10} kg
Volume-Equivalent Diameter of Secondary	0.150 km	0.451 km	0.168 km
Mass of Secondary	4.5×10^{9} kg	1.350×10^{11} kg	4.205×10^{9} kg
Mutual Orbit	...	...	...
Orbital Separation	1.189 km ($\sim 3.3 R_p$)	2.548 km ($\sim 3.9 R_p$)	0.980 km ($4 R_p$)
Eccentricity	0	0	0
Inclination relative to primary's equatorial plane	0°	0°	0°

2. We chose to fix initial mutual orbit conditions to narrow the parameter space and better isolate the specific contributions of planetary flybys and varying tidal-BYORP evolution parameters. Initializing the satellite in a singly synchronous, circular, equatorial orbit is a valid approach as it aligns with the typical characteristics of NEO binaries formed by fission from YORP spin-up. Initial simulations indicated that the effect of varying the starting mutual orbit semimajor axis is minimal on the final results, and is thus ignored. Further exploring different sets of initial mutual orbit configurations is left for future work.

Each system was run through the pre-processing block to identify NEOMOD migration pathways that came within some tolerance of their current observed heliocentric states (a_h, e_h, i_h) at any point throughout the evolution. We used initial tolerances of $\Delta a_h \leq 0.01$ AU, $\Delta e_h \leq 0.01$, and $\Delta i_h \leq 1°$ based on a similar NEO migration propagation study in Bottke et al. (2015, 2025). Didymos and Bennu were sifted a second time using arbitrary tolerances of $\Delta a \leq 0.002$ AU, $\Delta e \leq 0.002$, and $\Delta i \leq 0.2°$ to reduce the amount of matching pathways for effective analysis. In total, 103 pathways were found for Didymos (97 from the ν_6 source; 6 from the 3:1 source), 50 pathways for 1999 KW4 (44 from the ν_6 source; 6 from the 3:1 source), and 40 pathways for Bennu (36 from the ν_6 source; 4 from the 3:1 source).

4.2. Didymos results

The dynamical survivability of the Didymos binary was simulated along each matching migration pathway. Fig. 5 shows one representative pathway originating from the ν_6 resonance, corresponding to a ~4 Myr migration to Didymos's current heliocentric orbit, plotted in a_h–e_h and a_h–i_h space. The gray curve traces the migration pathway, black lines denote planet-crossing boundaries, the purple star marks the start of the migration pathway in NEO space, and the light pink star indicates the present orbit of Didymos. Circles mark planetary encounters (8 with Earth and Mars in this example).

The colorbar represents the probability that a test binary retains its satellite to the final state, assuming formation immediately prior to a given encounter. These probabilities are not computed per batch of 50 systems; rather, they reflect the fraction of binaries across all Monte Carlo iterations that survive each encounter or tidal-BYORP evolution segment relative to those reaching that stage. The overall survival probability along a pathway is obtained by multiplying the probabilities of all successive encounters and tidal-BYORP phases.

Because binaries must survive later encounters to reach the final configuration, the most recent encounters have the highest statistical confidence, while earlier stages have progressively lower sampling

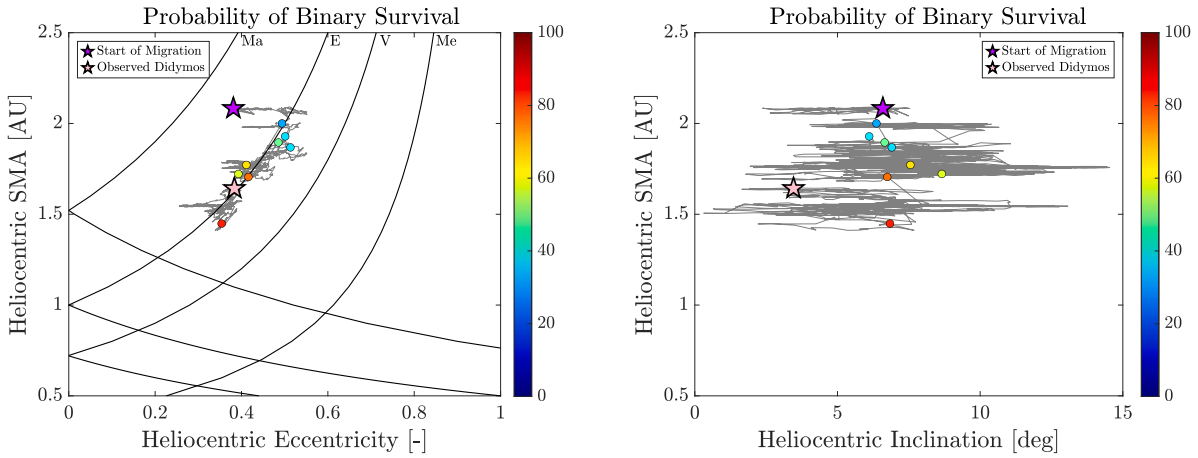

Fig. 5. Example migration pathway #1 (gray line), planetary encounters (circles), and probabilities for the Didymos system keeping a satellite in a_h versus e_h space (left) and a_h versus i_h space (right). The purple star is the start of the pathway, the light pink star is Didymos's observed heliocentric state, and the black lines in the left plot are the planet-crossing lines for Mercury (Me), Venus (V), Earth (E), and Mars (Ma). The colorbar represents the probability that a test binary retains its satellite all the way to Didymos's current heliocentric position, assuming the satellite formed immediately before the encounter of interest.

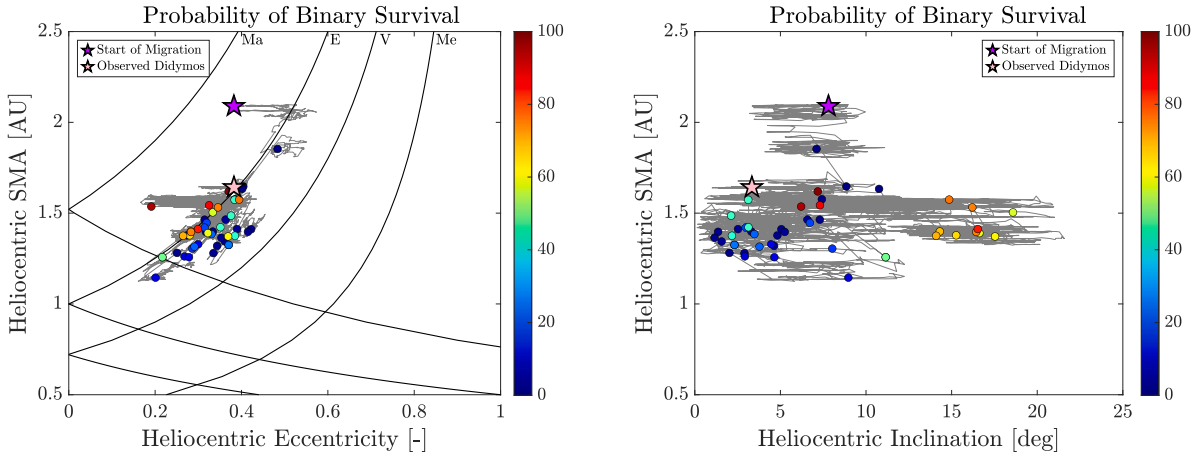

Fig. 6. Example migration pathway #2 (gray line), planetary encounters (circles), and probabilities for the Didymos system keeping a satellite in a_h versus e_h space (left) and a_h versus i_h space (right). The purple star is the start of the pathway, the light pink star is Didymos's observed heliocentric state, and the black lines in the left plot are the planet-crossing lines for Mercury (Me), Venus (V), Earth (E), and Mars (Ma).

statistics. Nevertheless, survival probabilities generally decrease backward along the pathway, so small differences at already low final survival rates are not significant. This approach also samples a broader distribution of mutual orbit geometries beyond the initially circular configurations.

For clarity, the first encounter (nearest the purple star) is light blue, indicating that 28% of binaries formed prior to that encounter survive all subsequent evolution to the final state. The final encounter (below the light pink star) is orange, indicating an 84% retention probability for satellites formed in that region.

It makes sense that the likelihood of survival increases the further the binary goes along its migration pathway. If binary systems experience fewer encounters, there is corresponding reduction in opportunities for their satellites to be stripped away during a flyby.

The very first encounter along a specific migration pathway is of particular interest, as it can be conceptualized as a "gateway" encounter between main belt and NEO space. It can be used to distinguish whether a binary system was formed back in the main belt or did not form until it was already in NEO space. If a binary formed prior to this first encounter is able to survive to the present-day observed heliocentric state, then it can be thought of as effectively having formed in the main belt. In this example, we find there is a ~30% chance of Didymos forming Dimorphos in the main belt based on our simulation statistics. It is important to establish that this probability (and all other provided probabilities) is only applicable to our simulated runs. In reality, we cannot assign an exact probabilistic percentage on the chance an asteroid formed its satellite in the main belt — we can only interpret that Didymos forming Dimorphos in the main belt is a plausible scenario. This logic is applicable to all other reported numbers throughout our results.

Fig. 6 shows a second migration pathway example for Didymos. It is evident that this pathway is quite different from Fig. 5. This trek is longer, with an approximate timescale of ~19 Myr, and the binary undergoes 47 planetary encounters, the vast majority of which are Earth flybys. Examining the first encounter, defined by the circle closest to the purple star, the likelihood of surviving from the main belt along this specific course is significantly lower compared to the first example. While before there was a nearly ~30% chance of surviving from the main belt, now it is <1%. We note again that this does not imply that these are the true survival probabilities. Rather, this just implies that the run with the higher survivability rate based solely on our sample statistics is more likely than the run with a near-zero rate to have formed a satellite in the main belt. This highlights how different migration tendencies can be for a given system.

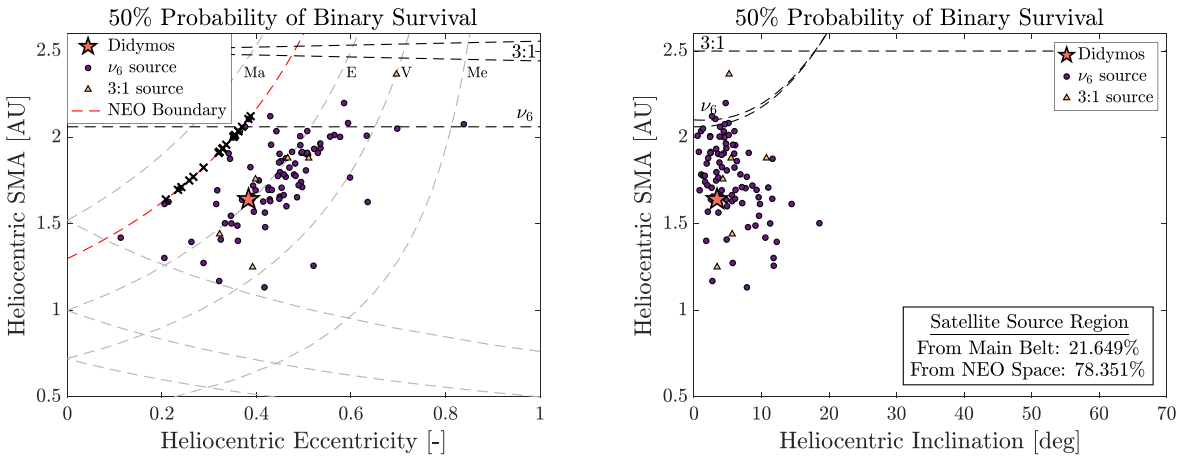

Fig. 7. The satellite-forming region for all survivability pathways with 50% chance of survivability to Didymos's current heliocentric state in a_h versus e_h space (left) and a_h versus i_h space (right). The red dashed line is the $q_h < 1.3$ AU boundary between main belt and NEO space. The dashed black lines spatially mark the heliocentric locations of the ν_6 and 3:1 resonance sources. Each marker shows the initial locations where newly-formed satellites have a 50% probability of surviving to the final Didymos heliocentric state. Purple circles represent migration pathways from the ν_6 resonance source and tan triangles represent pathways from the 3:1 resonance source. The dashed gray lines in the left plot are the planet-crossing lines for Mercury (Me), Venus (V), Earth (E), and Mars (Ma). The black "X" marks in the left plot symbolize the number of cases whose 50% survival threshold was the first encounter, indicating that those systems could have formed in the main belt. One "X" corresponds to all test binaries that form the probabilities for a single migration route. The right plot also presents the probability of Didymos forming Dimorphos in NEO space or back in the main belt.

Among all migration pathways for Didymos, the minimum and maximum number of encounters per a single pathway are 0 and 944, respectively, with a median of 10 encounters.

These two example migration trajectories demonstrate that there is no singular highway to transition from the main belt to NEO space. While some may share similarities, others may exhibit wildly different behaviors. Thus, while it is important to consider and evaluate the migration pathways in our NEOMOD dataset, the reader should keep in mind that we will never precisely know what happened to the binary asteroid in question.

Fig. 7 visualizes the results of all 103 matching migration pathways that arrive at Didymos's heliocentric orbit at some point during its time history. The purple circle and tan triangle markers show the initial locations where a satellite formed somewhere in heliocentric space has a 50% probability of surviving to reach Didymos's current heliocentric state. Each marker represents an individual pathway. If a binary fails to reach a 50% likelihood of survival, it is not plotted. The purple circles represent those coming from the ν_6 resonance, while the tan triangles are from the 3:1 resonance. They can be considered the bounding region of space where one can expect an asteroid to form a satellite and keep it to the existing Didymos heliocentric orbit. The 50% survivability threshold was chosen arbitrarily, but it serves as a practical benchmark for identifying the point at which dynamical survival becomes more likely than not.

The black "X" marks in the a_h versus e_h plot are solely a visual representation of migration pathways whose 50% survivability threshold corresponds to the first encounter, indicating the binary system formed in the main belt. (Note we are referring to the first possible encounter in the entire migration route, not every "first" encounter where a batch of 50 test binaries is initialized in each iteration of the Monte Carlo loop.) The marks are placed along the NEO boundary line to symbolize this interpretation. Therefore, a little over a fifth of simulated cases that made it to Didymos's observed state came from the main belt, according to our 50% survivability rate threshold. Again, this just implies that it is plausible that Dimorphos was formed in main belt space.

We can also use our model to analyze the final binary orbit parameters of the surviving test binaries. Fig. 8 shows the final surviving mutual orbits as a function of semimajor axis, eccentricity, and inclination. We again use the 50% survivability threshold for these plots.

Starting from the initial condition where all test binaries have zero mutual eccentricity and inclination, the surviving binaries display a broad range of final parameters, with distributions spanning several orders of magnitude. Blue dots represent satellites that are dynamically relaxed in their final state, meaning there was enough time for tides to damp out libration. Red dots are satellites that did not dynamically recapture from tides and remained tumbling in their final state. The fact that both exist in Fig. 8 indicates that our model can form both synchronous and wide, asynchronous, eccentric binaries. Each state can be found in observed binary systems. Examples include the singly-synchronous systems 1999 KW4 (Ostro et al., 2006) and 1996 FG3 (Scheirich et al., 2015), and the tumbling satellite of 1991 VH (Pravec et al., 1998, 2016; Meyer et al., 2024).

We note that the some of the wider binaries observed in our results have synchronous satellites. This is simply a byproduct of our model assumptions, where we do not allow the satellite to start tumbling from joint tidal-BYORP expansion. In reality, tidal strength would significantly drop off at these distances and the likely outcome would be that the satellites enter a tumbling state, pausing BYORP evolution.

Our model results successfully replicate the observed binary parameters of the pre-DART impact Didymos system. This is evident from the gold star and line in both plots, which lie within the main distributions of the simulated binaries. We did not explicitly control the final binary orbit to converge to the current state of Didymos, which is why we see the large spread in final orbit parameters. It is interesting to note that many surviving systems are similar to real systems, but at the same time there are a number of results that are quite a bit different, such as wider or highly inclined systems. These differences could be the focus of future work. Additionally, we note that even though test binaries are initialized with a fixed binary semimajor axis, it was found that varying this parameter does not drastically influence the statistics. This is due to the tidal-BYORP equilibrium semimajor axis being the main driver for survivability, which is independent of initial semimajor axis but largely dependent on B and k/Q (which we do vary). This observation will be discussed in further detail in Section 4.5.

Another notable item in Fig. 8 is the presence of a large population of test binaries with highly inclined mutual orbits relative to the primary's equatorial plane. Only semimajor axis and eccentricity are affected by tides and BYORP in our model, so these high inclination values are the byproduct of successive planetary encounters. Curiously,

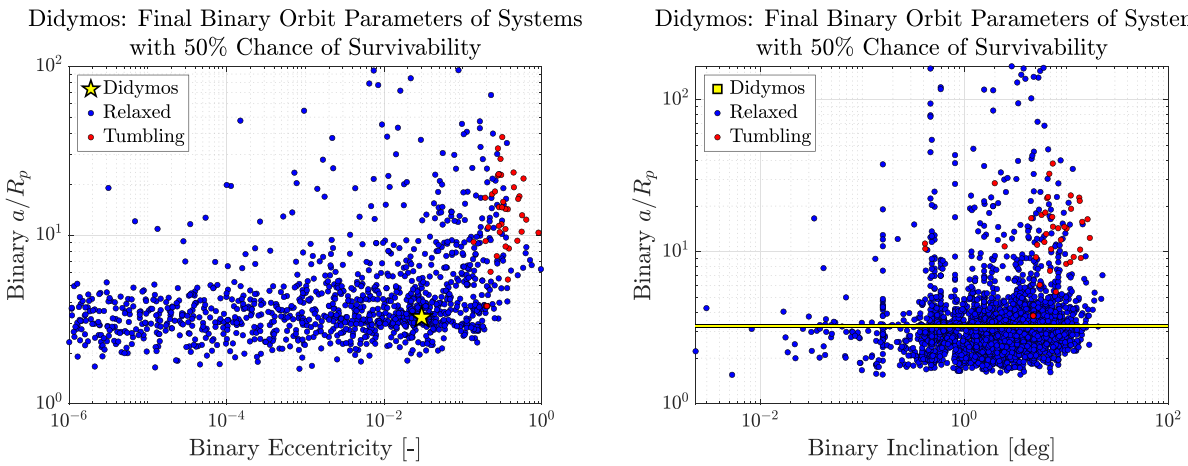

Fig. 8. Final binary mutual orbit parameters of surviving simulated systems with 50% chance of keeping a satellite to the final Didymos heliocentric state as a function of binary mutual orbit separation versus eccentricity (left) and separation versus inclination relative to the primary's equatorial plane (right). The blue markers indicate dynamically relaxed systems that reach the final state, and red markers indicate tumbling systems. The gold star represents the pre-impact values of Didymos and Dimorphos reported in Table 1. Note that we plot a horizontal yellow and black line to represent binary inclination since this value is unknown but assumed near zero in prior studies.

most of the observed binary NEO and SMBA systems are coplanar with the primary's equator, contradicting our results (Ostro et al., 2006; Scheirich and Pravec, 2009; Pravec et al., 2012; Pravec and Scheirich, 2012).

We believe this mismatch can be explained by one of two possibilities. The first is that we are simply missing a mechanism in our model that is capable of effectively damping orbit inclination. This possibility warrants further investigation in future modeling efforts.

The second option is that a broader range of binaries with high inclinations exists, but they are significantly harder to detect due to observational biases favoring low-inclination systems. One of the main techniques used to detect NEO and SMBA satellites are ground-based photometric light curves. This technique measures the brightness of the system and detects dips in overall brightness during eclipses between the two opponents or occultations relative to the observer's line of sight, indicating the presence of a satellite (Pravec et al., 2006). The challenge with this method is that it requires a favorable geometric alignment with the Earth and Sun (Pravec et al., 2006). Specifically, it is beneficial for the obliquity of the mutual orbit plane relative to the ecliptic to be near 0° or 180°, such that the orbit is edge-on with the Sun and Earth (Pravec et al., 2012).

Radar is not inherently biased against wide or inclined binaries (Vavilov et al., 2022) and has detected dozens of near-Earth systems (Margot et al., 2015). However, resolving both components requires close Earth approaches (<0.2 AU) (Ćuk, 2007; Margot et al., 2015), and wide binaries may be disrupted before such encounters occur (Bottke et al., 1994; Walsh and Richardson, 2008; Fang and Margot, 2011a). Radar does not rely on mutual events, but constraining inclination relative to the primary's equatorial plane requires knowledge of the primary's spin pole, which is often degenerate from a single apparition. Reliable spin-state solutions typically require multiple apparitions and supporting light-curve data (Margot et al., 2015; Benner et al., 2015), and assumptions about pole alignment are sometimes adopted based on expected formation mechanisms (e.g., rotational fission; Naidu et al. 2015).

Accordingly, if we have binary systems where the primary equator is near the ecliptic plane, high inclination mutual orbits excited by flybys could potentially disrupt the orientation required to detect these systems using light curve methods. This possibility is supported by indirect evidence of a missing population of wide asynchronous binaries. Recent crater studies have reported that the properties of doublet craters observed on Ceres, Vesta, and Mars suggest a larger population of well-separated and inclined binaries that does not agree with the known binary population (Vavilov et al., 2022; Herrera et al., 2024). While Ceres and Vesta cannot be used as justification for the inclined cases we observe from flybys with the inner planets (since they would require a different inclination excitation mechanism in the main belt), Mars could lend credence to inclination pumping from planetary encounters. Resolving the mystery behind this population discrepancy is left for future work.

4.3. 1999 KW4 results

The dynamical survivability of the 1999 KW4 system was also simulated along every matching migration pathway identified. We again look at two examples from the ν_6 resonance source, as that is where most of the matching pathways reside. They are shown in Figs. 9 and 10.

Similar to the two Didymos examples, we can see that each of the 1999 KW4 pathways are unique in behavior. Unlike Didymos, the 1999 KW4 pathways exhibit a near-zero chance of keeping a satellite along most of its migration pathway until closer to the end of the pathway. It stands to reason that a 1999 KW4 satellite would not survive all the way from the main belt, given that its orbit deep in NEO space exposes it to a greater number of encounters that it would need to withstand.

The pathway in Fig. 9 has a timescale of ~53 Myr with 642 encounters, while the pathway in Fig. 10 has an even longer timescale of ~88 Myr with 675 encounters. Among all 1999 KW4 migration pathways, the minimum, median, and maximum number of encounters experienced are 180, 507, and 1474, respectively. Given the orders of magnitude increase in encounters on average compared to Didymos, it is highly unlikely that 1999 KW4 could have formed a satellite in the main belt.

Furthermore, there is a significant portion of NEO space where it is unlikely that 1999 KW4 formed. Many of the migration pathways include a small number of extremely close planetary flybys (~1.5–2 planetary radii) that consistently disrupt 100% of the test binaries encountering them. These close flybys act as highly effective gatekeepers, limiting survivability in specific regions of NEO space.

By comparing the Didymos and 1999 KW4 individual pathway results, we can see that in addition to there being a multitude of migration possibilities for one body, different bodies in different zones in NEO space have drastically different outcomes. This difference is evident from Fig. 11, which shows the result of all 50 matching migration pathways that arrive at 1999 KW4's heliocentric orbit at some point during its time history. The bounding region of forming a satellite with

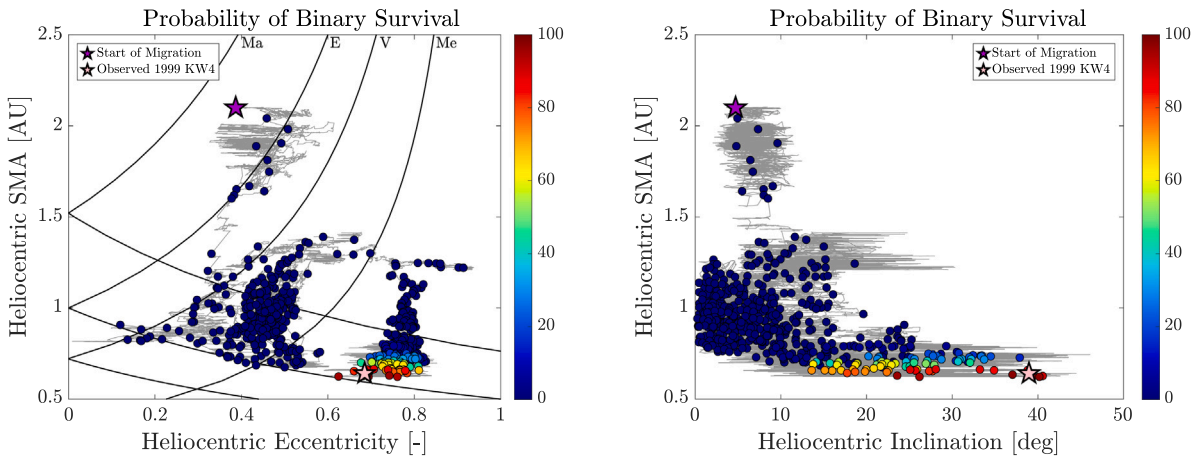

Fig. 9. Same as Fig. 5, but for 1999 KW4.

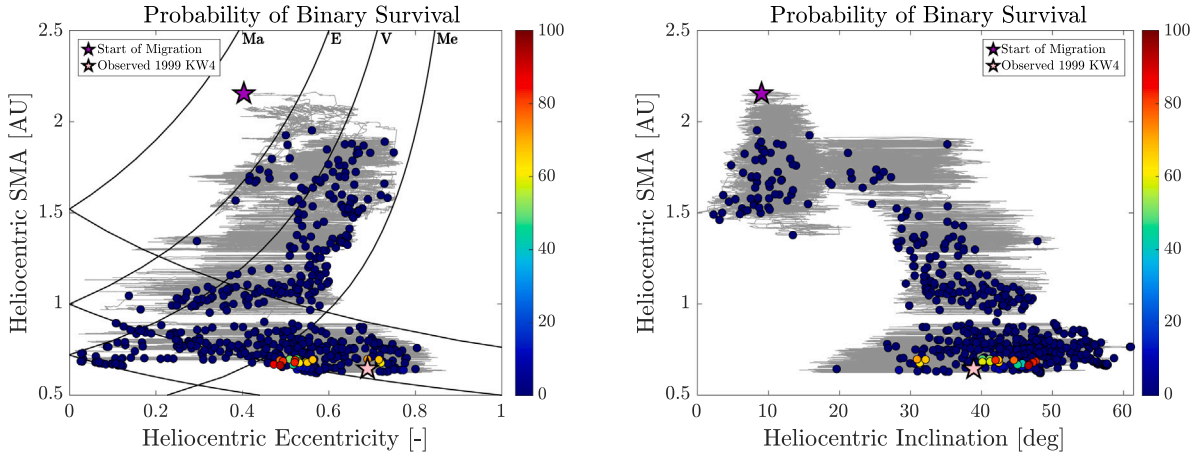

Fig. 10. Same as Fig. 6, but for 1999 KW4.

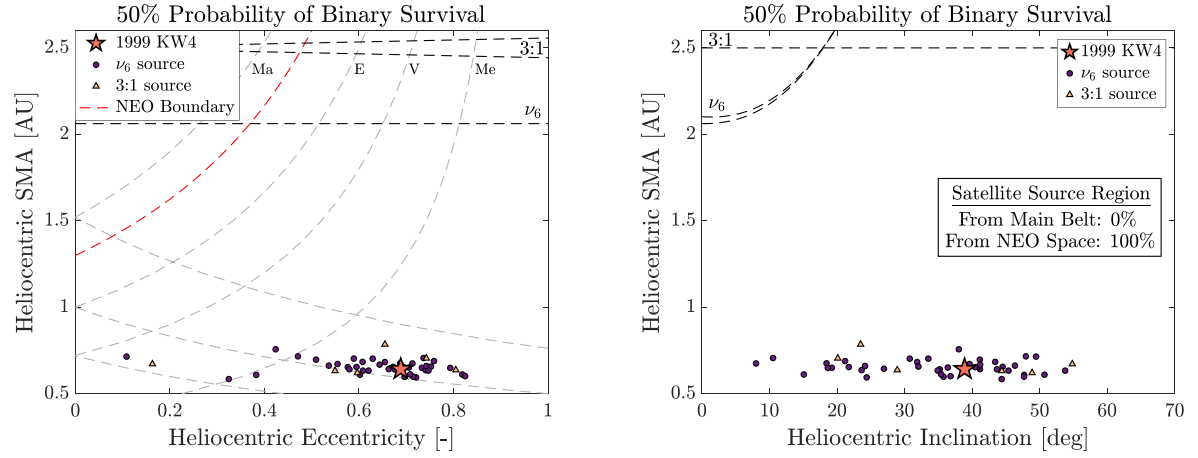

Fig. 11. Same as Fig. 7, but for 1999 KW4.

a 50% chance of surviving to 1999 KW4's current heliocentric state is more limited than that of Didymos.

Fig. 11 also reveals that, although there is a spread of potential satellite-forming heliocentric eccentricities and inclinations, satellites have no realistic chance of survival unless they form within approximately 0.2 AU of 1999 KW4's current heliocentric semimajor axis. Looking at the first encounter for each pathway, there is a 0% chance of 1999 KW4 forming and keeping its satellite from the main belt, based on our simulation statistics.

Our statistics are limited to the simulated cases and the sample size of 50 test binaries initialized per encounter. We expect the overall trends to persist with a larger sample. Furthermore, the model does not weight results by the observed distribution of binaries in heliocentric space. Thus, if a binary is observed in a bin where our simulations

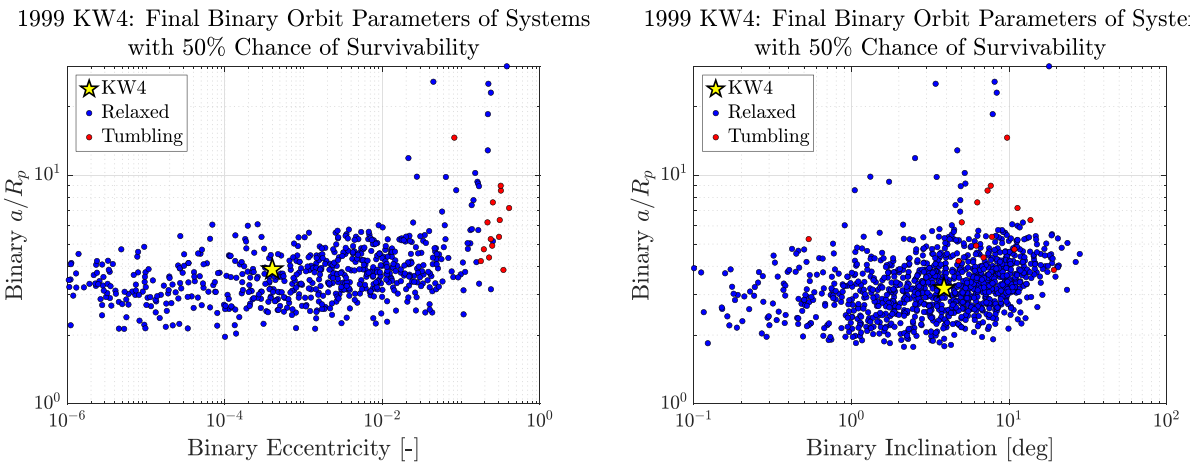

Fig. 12. Same as Fig. 8, but for 1999 KW4.

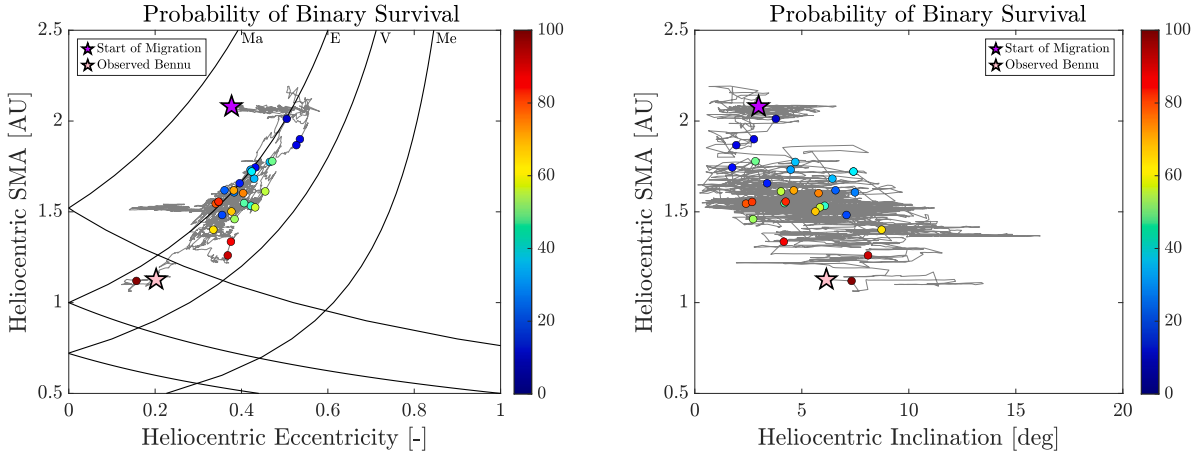

Fig. 13. Same as Fig. 5, but for Bennu with a prescribed satellite.

predict negligible survival from the main belt, this does not definitively imply formation in NEO space; rather, it may reflect sampling limitations. Accordingly, our results indicate only that formation in NEO space is more likely than formation in the main belt.

Analyzing the final binary orbit parameters of the systems with 50% survivability probability, Fig. 12 shows that we can successfully reproduce the current configuration of 1999 KW4's mutual orbit starting from the initial conditions of a planar circular orbit. Similar to Didymos, there is a large population of more inclined binaries, providing further data to support either an absent inclination-damping mechanism or a missing population of wide, inclined binaries. Unlike Didymos, however, there are fewer tumbling binaries. This could be attributed to a combination of tidal recapture and distant/weak planetary encounters. One plausible scenario is that sufficient time exists for tidal forces in the binary system to dampen satellite tumbling after the final planetary encounter, allowing the system to settle into 1999 KW4's final state. Another possible situation is that the satellite starts tumbling due to an intermediate planetary encounter, has enough time to recapture in a subsequent tidal-BYORP evolution leg, and then experiences a series of weak planetary encounters that do not re-trigger the tumbling state. We note again though, that the widest final orbits shown in Fig. 12 would likely experience satellite tumbling at those distances if such dynamics were accounted for in our model.

4.4. Bennu results

The dynamical survivability of Bennu with a prescribed pseudo-satellite at a binary semimajor axis of $4R_p$ was simulated along every matching migration pathway identified to assess the likelihood of satellite loss. Like the two existing binary systems assessed, we also present two representative migration pathways from the ν_6 resonance source to evaluate migration behavior.

The first pathway is shown in Fig. 13. It shows a ~7 Myr migration pathway largely following the Earth-crossing line and experiencing 29 Earth encounters. These successive Earth encounters cause Bennu to migrate along lines of constant Tisserand invariant with respect to Earth, with the test Bennus ultimately converging to Bennu's observed orbit, characterized by low semimajor axis and eccentricity values (Bottke et al., 2025).

The second pathway in Fig. 14 shows a longer ~21 Myr pathway with 225 planetary encounters. Compared with the first example, this pathway experiences encounters with all four of the inner planets, rather than just with Earth. This pathway is more similar to the 1999 KW4 example, where the probability of survival is near-zero until the end of the pathway.

Among all Bennu migration pathways, the minimum, median, and maximum number of encounters experienced are 17, 43, and 226, respectively. These values imply that Bennu undergoes a similar number of encounters to Didymos on average. For some pathways, however, it experiences hundreds of additional encounters, resembling those of 1999 KW4 (and a few outlier cases for Didymos).

Fig. 15 shows the result of all 40 matching migration pathways from Bennu from the ν_6 and 3:1 resonance sources, marking the bounding region for the 50% survivability threshold. The Bennu trends are similar to Didymos in that we see a wider spread in the allowable region where

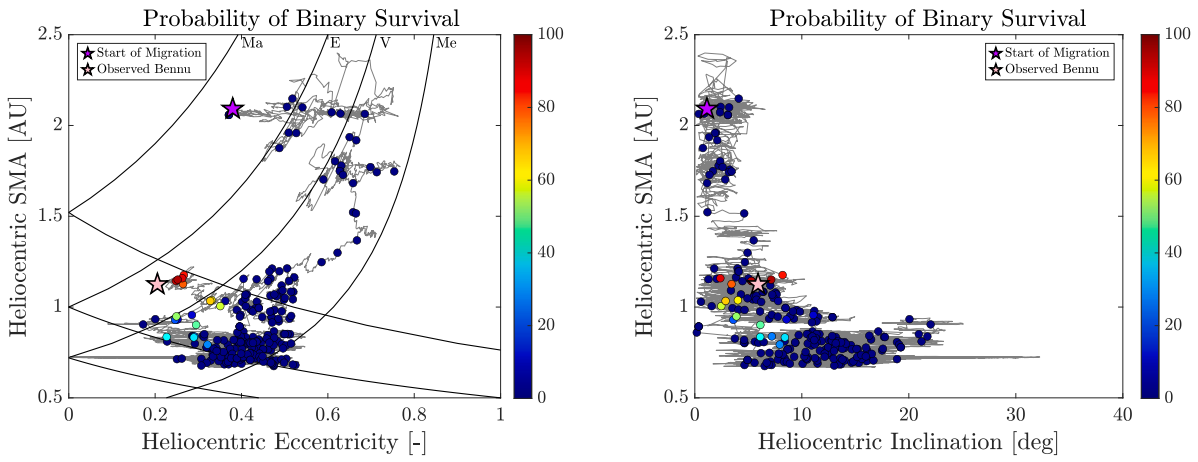

Fig. 14. Same as Fig. 6, but for Bennu with a prescribed satellite.

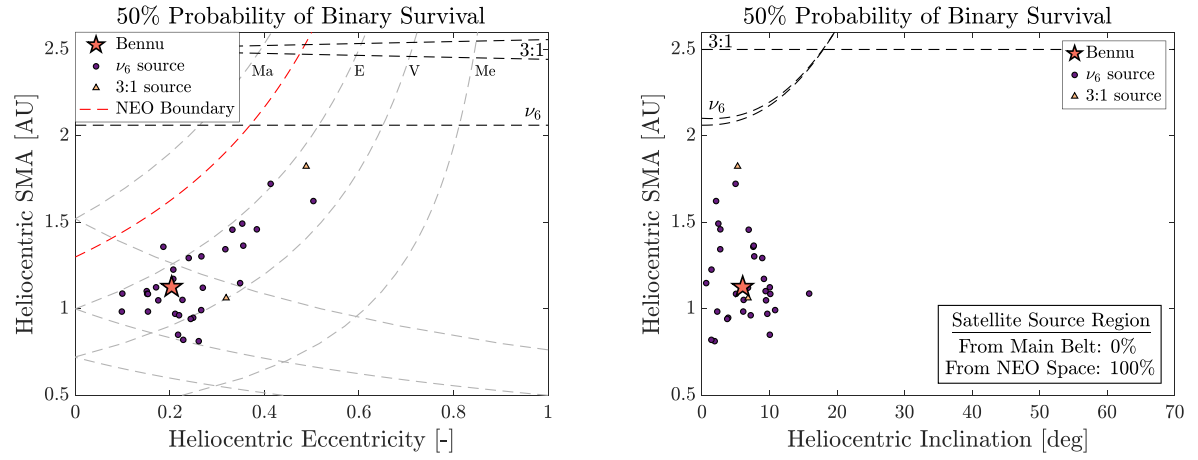

Fig. 15. Same as Fig. 7, but for Bennu with a prescribed satellite.

Bennu is likely to have formed a satellite in (a_h, e_h, i_h) space. Unlike Didymos, but similar to 1999 KW4, none of the simulated cases for Bennu survived from the main belt.

4.5. Lifetimes of surviving systems

Fig. 16 shows the bounding regions of 50% probability of surviving to existing binary states for all three systems on a single plot for further comparison. For the sake of comparison, each system and corresponding location markers from the two sources regions have their own color. While there is slight overlap in the formation region of Didymos and Bennu, the results show that the three systems likely form their satellites in distinctly different regions of space. 1999 KW4's satellite formation is confined to the smallest a_h values of the three systems, but experiences the widest range of e_h and i_h values. While Didymos and Bennu have larger distributions in a_h, Bennu's current position is at a lower a_h and e_h compared to Didymos and the formation region does not extend back into main belt space.

We conclude that it is relatively unlikely for a main belt binary to survive for an extended period in NEO space today unless the system is relatively new to an Earth-crossing orbit (i.e., it has undergone only a small number of planetary encounters). Typically, this would imply that its perihelion is close to or greater than the Earth-crossing threshold, and its semimajor axis is near 2 AU.

One interpretation of this result is that the low survival rates from the main belt implies a larger fraction of main belt binaries to get the known 15% binarity fraction in NEO space. Although it is suspected that the small main belt binary fraction is also roughly 15% (Pravec et al., 2012, 2016; Pravec, 2025), this estimate is more uncertain than NEO binaries since these bodies are harder to detect. On the other hand, if the binary fraction truly is the same among NEO and SBMA populations, then it is unlikely that main belt binaries are a huge source for NEO binaries.

Fig. 16 also provides the ages of the satellites formed for all three systems that have a 50% probability of survivability. 1999 KW4 and Didymos have relatively similar age distributions, with values ranging from minima on the order of 10^3–10^5 years to maxima of ~10^7 years. The median ages of the surviving 1999 KW4 and Didymos satellites are ~2 Myr and ~1.2 Myr, respectively.

The surviving pseudo-satellites of Bennu experience an order of magnitude smaller possible ages, ranging from 10^4 to 10^6 years with a median age of ~570,000 years. This corroborates the hypothesis that Bennu could have been a top-shaped primary of a YORP-formed binary at some instance in its dynamical history (Walsh, 2018; Bottke et al., 2025). Our simulated lifetimes suggest that if Bennu at one point had a satellite, it would need to have been dynamically younger compared to the other two systems for it to exist today.

With shorter survival times, Bennu has a longer window during its migration history to lose a satellite. This aligns with the general stability trends of binaries, where systems with either wide mutual orbits or long mutual orbital periods tend to be less stable. Bennu has the smallest diameter and mass among the three primaries, resulting in a weaker gravitational parameter and correspondingly longer mutual orbit period for a given binary semimajor axis. This means that Bennu

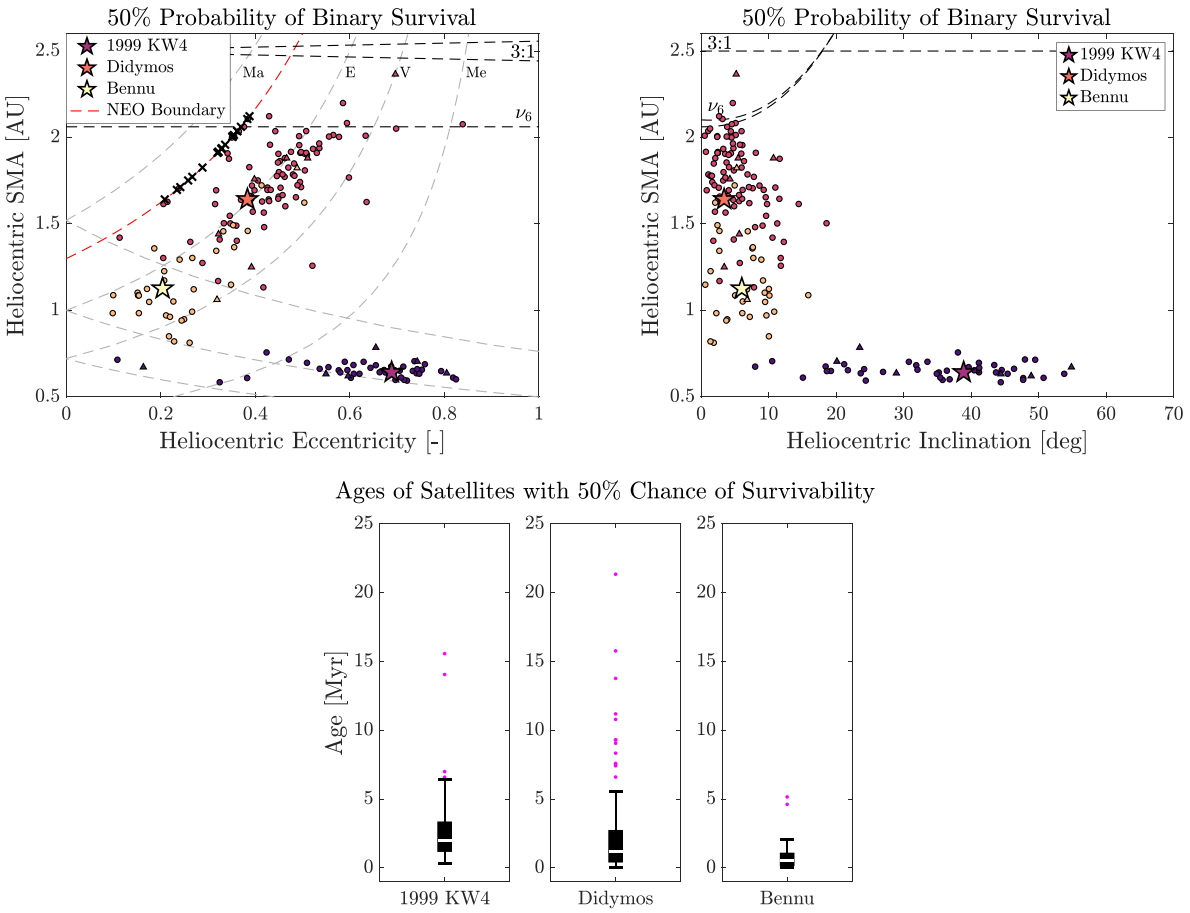

Fig. 16. The satellite-forming region for all survivability pathways with 50% chance of survivability to the current heliocentric states of Didymos, 1999 KW4, and Bennu in a_h versus e_h space (top left) and a_h versus i_h space (top right). The red dashed line is the $q_h < 1.3$ AU boundary between main belt and NEO space. The dashed black lines spatially mark the heliocentric locations of the ν_6 and 3:1 resonance sources. Each pink, purple, and tan marker shows the initial locations where newly-formed satellites have a 50% probability of surviving to the final Didymos, 1999 KW4, and Bennu heliocentric states, respectively. Circles represent migration pathways from the ν_6 resonance source and triangles represent pathways from the 3:1 resonance source. The dashed gray lines in the left plot are the planet-crossing lines for Mercury (Me), Venus (V), Earth (E), and Mars (Ma). The black "X" marks in the left plot symbolize the number of Didymos cases whose 50% survival threshold was the first encounter, indicating that those systems could have formed in the main belt. The ages of satellites with 50% chance of survivability for all three systems (bottom).

has a lower binding energy for its mutual orbit and therefore its test satellites are more susceptible to disruptions at tighter mutual orbit separations from planetary encounters.

It is important to note that the overall ages of surviving satellites for our model systems are much longer than previously suggested. Prior estimates of NEO binaries place BYORP-driven disruption timescales at 10^5 years at 1 AU (Ćuk, 2007; Ćuk and Nesvorný, 2010), matching the minimum ages from our simulations.

Conversely, we also report binary lifetimes spanning several million years. This extended longevity is attributed to the theoretical tidal-BYORP equilibrium mechanism. The equilibrium occurs when expansive tidal forces and the contractive effects of BYORP balance each other. This stabilizes the mutual orbit at the equilibrium semi-major axis defined in Eq. (6). This state is hypothesized to persist for timescales $>10^6$ years (Wang and Hou, 2021), or potentially indefinitely until broken apart by an external collision or close planetary encounter (Jacobson et al., 2016).

Table 3 reports the breakdown of BYORP coefficients and tidal parameters corresponding to surviving systems. Specifically, the magnitude and sign statistics are for test binaries with 50% chance of having a surviving satellite to the final heliocentric state of the observed system. While no apparent dynamical correlations exist for the magnitudes of B and k/Q values, there is a clear trend for the sign of the BYORP coefficient. While some satellites were able to survive with a positive BYORP coefficient, the vast majority of surviving test binaries possess a negative BYORP coefficient, attesting to the dependence on the theoretical long-term stability of the tidal-BYORP equilibrium configuration.

The existence of a long-lived tidal-BYORP equilibrium carries additional implications, particularly concerning the tidal de-spinning of the primary. If this equilibrium is indeed operating over the timescales suggested by our model, it implies that significant spin-down of the primary should occur as tidal forces gradually act to synchronize its rotation with the mutual orbit. This process would unfold over timescales several orders of magnitude longer than the rapid evolution driven by BYORP (Ćuk, 2007; Goldreich and Sari, 2009; Ćuk and Nesvorný, 2010). Consequently, our model predicts that we should observe primaries with slower spin rates. In contrast to this prediction, nearly all primaries in known NEO and SMBA binaries are observed to be rapid rotators. This gives rise to several potential hypotheses and different ways to interpret the observed data.

For example, if we observe a rapidly rotating single asteroid such as Bennu, it could suggest it experienced the early loss of a satellite in its dynamical history, thereby preventing tidal dissipation from significantly slowing the primary's spin period. Conversely, if significant tidal spin-down of primaries is expected for older satellites, the presence of fast-spinning primaries in known binary systems could serve as evidence for the dynamical youth of the satellite.

Table 3
Statistical breakdown of B and k/Q values for surviving systems.

System	$\lvert B\rvert = 10^{-3}$	$\lvert B\rvert = 10^{-2}$	$\lvert k/Q\rvert = 10^{-6}$	$\lvert k/Q\rvert = 10^{-5}$	Positive B	Negative B
Didymos	55.297%	44.703%	52.112%	47.888%	14.996%	85.004%
1999 KW4	49.413%	50.587%	53.568%	46.432%	2.349%	97.651%
Bennu	49.867%	50.133%	51.194%	48.806%	2.520%	97.480%

These interpretations are complicated by interactions with YORP cycles on the primary, possibly confounding our understanding of the relative importance of contributing torques. It is possible that YORP spin-up must remain active to counterbalance tidal de-spinning in these long-term stable systems. This idea might be supported by the observation that, among all currently detected cases of YORP, all but one involve spin-up (Ďurech et al., 2024; Feng et al., 2025), and hints that transversal conduction of heat in small-scale surface irregularities breaks symmetry between rotational acceleration and deceleration (Golubov and Krugly, 2012; Golubov, 2017). Thus, YORP is, at times, confusing and therefore it is very possible that by extension the field's understanding of BYORP is far from complete.

A potential caveat to this trend could be an observational bias against detecting decreasing spin rates (Feng et al., 2025). Alternatively, it is possible that tidal dissipation is several orders of magnitude weaker than currently anticipated, meaning that its ability to slow down the primary's spin would be negligible. Another possibility is that the tidal-BYORP equilibrium is not as strong as current studies suggest. If this mechanism is indeed weaker, binary system lifetimes would likely decrease accordingly. We pose these questions as avenues for further investigations.

5. Discussion

5.1. The dynamical uniqueness of didymos

Our results for Didymos, 1999 KW4, and Bennu suggest that Didymos is the only system that has some likelihood of having formed its current satellite in the main belt. The next question to ask is whether our conclusions make sense given the observed properties of the Didymos system.

Recent work suggests that the Didymos binary is a special end member of the known binary NEO population. For example, it has one of the tightest observed mutual orbits and one of the fastest primary rotation rates, as well as Didymos and Dimorphos being some of the least elongated primaries and secondaries (Pravec, 2025). This suggests that our dynamical survivability findings for Didymos may not be representative of other Apollo-class systems that have made similarly limited excursions into NEO space. Perhaps our 1-in-5 likelihood for retaining a Didymos satellite from the main belt is merely a product of Didymos's distinct dynamical characteristics.

Additionally, specific surface features on Dimorphos, such as a paucity of dusty regions (Lucchetti et al., 2024; Vincent et al., 2024) and craters (Barnouin et al., 2024) imply it has a younger surface than Didymos. This could indicate that the satellite is so dynamically young that it could not have formed in the main belt. On the other hand, these missing surface features might simply be a consequence of other processes that have reset Dimorphos's surface in the recent past (e.g., impacts producing seismic shaking, non-principal axis rotation, or ejecta from Didymos landing on Dimorphos; Richardson et al., 2020; Agrusa et al., 2022; Barnouin et al., 2024; Stern, 2009).

5.2. Limitations of current study

There are many simplifying assumptions made in our model that can be expanded upon in future versions of the model. For example, we use k/Q values spanning two orders of magnitude due to the significant uncertainty surrounding the strength and mechanical properties of rubble piles in the literature. Recent work suggests that k/Q could be several orders of magnitude higher than the range used in this work (as high as 10^{-2}; Burnett et al., 2024).

As a second example, consider that Ćuk et al. (2024) suggests that rubble piles may be dominated by short bursts of dissipative behavior rather than continuous tidal evolution, whereas Efroimsky (2015) argues that dissipation could be dominated by viscosity, rather than a classical friction-based approach with a single k/Q value. Although our understanding of the actual behavior of these bodies is limited, future models should, at a minimum, explore a broader range of tidal parameters to better capture potential outcomes.

We also note that the tidal-BYORP analytical equations used in our model have a limited scope in how they treat binary evolution. If BYORP is contractive, the equations will always enforce a tidal-BYORP equilibrium endpoint by Eq. (6), and our chosen magnitudes for B and k/Q values do not allow for the formation of contact binaries. We would instead need to incorporate B values stronger than 10^{-2} and k/Q values weaker than 10^{-6} to get a tidal-BYORP equilibrium semimajor axis less than the Roche limit.

At present, the only way to form a contact binary in our model is through planetary encounters. Furthermore, joint tidal-BYORP expansion is unbounded in our model until the satellite escapes the system. In high-fidelity modeling of tidal-BYORP evolution, tidal dissipation strength drops off significantly at wide separations and would cause the satellite to enter a tumbling state (Cueva et al., 2024). This would shut off BYORP and pause secular evolution before the satellite would have a chance to escape. Our model currently accounts only for tidal recapture. If we were to add the ability to initiate tumbling at specific distances, we would expect the binaries to have an increased survivability rate. Note that previous studies show that BYORP can expand a satellite to the Hill sphere before losing synchronous lock, so allowing for satellite disruption from BYORP expansion is not an unfounded outcome and thus a reasonable assumption (McMahon and Scheeres, 2010a; Jacobson et al., 2013). Furthermore, this preliminary model cannot capture all possible perturbations a binary may experience. As the binary expands closer to the Hill sphere, it is likely that additional perturbations not included in our model will trigger the final unbinding of the two components. Nevertheless, expansive BYORP is what drives the orbit to susceptibility for destruction. Therefore, attributing the final disruption to BYORP is a reasonable simplification for the purposes of this study.

Our approach to modeling planetary flybys could also be improved by numerically propagating the orbital dynamics during a flyby, rather than using a probabilistic analytical approach. Currently, we compute the average change in Keplerian mutual orbit elements from the flyby and assign equal chance of increasing or decreasing those values. This approach does not adequately account for the influence of binary orbit orientation when entering a planetary encounter. Previous studies have shown that the incoming binary geometry as the system approaches the planet may influence how the system responds to the encounter (Bottke and Melosh, 1996; Meyer and Scheeres, 2021). Additionally, we assume a 100% disruption rate for encounters with sufficiently large flyby parameters. This assumption is a modest over-estimate; higher-fidelity GUBAS simulations suggest that even very close planetary encounters can have small probabilities of survival, which would likely increase overall survivability rates.

We also assume that a satellite forms instantaneously prior to undergoing the initial encounter in a sequence. We do not account for formation of a satellite along the arc of the migration pathway prior to

the location of the initial encounter, negating any dynamics that could affect the orbit preceding the first encounter.

While our binary simulations end once the satellite is lost, in reality we can expect the primary to form new satellites. This formation-destruction cycle of binaries is expected to form satellites several times throughout the rubble pile's dynamical lifecycle (Ćuk, 2007; Jacobson and Scheeres, 2011a). While it is much easier to strip the satellite from the primary rather than tidally disrupt an asteroid and form a satellite during a close planetary flyby (Walsh and Richardson, 2008), it is possible for multiple YORP spin-up cycles to occur, leading to several instances of satellite formation. However, the main focus of this paper was to assess how long certain satellites survive. Thus, successive formations of satellites can be viewed as a different question our tool could be used to answer, rather than a caveat of the presented work.

Additionally, our model does not account for satellite libration, nor does it track the spin rates of the system's components. The spin rate of the primary could be easily added to our model to further explore interactions between tidal spin-down and combating YORP spin-up over long durations. Furthermore, future work will explore a wider range of initial conditions for the mutual orbits of test binaries, including configurations with non-zero eccentricity and inclination.

Our model also does not include satellite acceleration caused by unbalanced thermal cooling and heating following the entry and exit of the primary shadow, dubbed the Yarkovsky–Schach (YS) effect (e.g., Vokrouhlický et al., 2005; Zhou et al., 2024; Zhou, 2024). While potentially important, the YS effect depends on another set of poorly constrained variables, opening the problem of a potential over-parametrization of our results. We thus postpone extension of our model by the YS effect to the future studies.

Finally, we only test one plausible size ratio for the prescribed pseudo-satellite of Bennu. In theory, a larger satellite will tend to have a weaker BYORP coefficient due to factors like bulk shape becoming more spherical and less irregular as size increases. This would widen the tidal-BYORP equilibrium semimajor axis, making a larger satellite more likely to be stripped. A size ratio optimized for satellite survival could hypothetically be assessed, but in general smaller satellites (including our the prescribed radius we use) fall within the low mass ratio regime (defined by secondary-to-primary mass ratios below 0.2, representative of the binary systems described throughout this study; Jacobson and Scheeres, 2011a). Thus, we anticipate smaller satellites to generally produce similar outcomes, making our choice of pseudo-satellite a reasonable starting point.

Ultimately, approximations and reasonable assumptions were made in order to make this preliminary study computationally tractable.

5.3. Extensions of current study

Beyond investigating the dynamics of existing NEO binary systems, our tool offers numerous opportunities for exploration in other areas. One direction is the formation and evolution of escaping ejecta binaries (EEBs). These binary systems form as a result of catastrophic collisions where escaping fragments become gravitationally bound (Durda et al., 2004). They have different characteristics than typical NEO binaries, such as larger component mass ratios and wider, eccentric, and inclined mutual orbits. To date, however, very few candidate EEBs have been identified in the main belt (Durda et al., 2010; Polishook et al., 2011), and none have been detected in NEO space. This is despite the model prediction that numerous EEBs should be created in asteroid family-forming events (Durda et al., 2004; Nesvorný et al., 2006; Minker et al., 2025). Our model could be used to examine this discrepancy and potentially explain the dynamical history of EEBs. It may even be able to predict where they should exist today, if some can dynamically survive. Such work could also be connected to the disagreement between the properties of known binary NEOs and SMBAs and the differing characteristics of doublet craters observed on Ceres, Vesta, and Mars (Vavilov et al., 2022; Herrera et al., 2024).

The formation of asteroid pairs – escaped bodies previously bound by a mutual orbit now on alike orbits about the sun – could also be another line of possible inquiry. The dynamics of these systems can be backwards integrated to determine their age since separation (Pravec et al., 2010, 2019; Pou and Nimmo, 2024). We could perform an in depth comparison between known asteroid pair formation timescales and the disruption timescales of test binaries in our dynamical model to assess if there are preferential pathways from the main belt responsible for the formation of asteroid pairs. This could be tied with a study performing the opposite analysis of what is reported in this work. Rather than looking at the timescales of survival for systems with known satellites, we could look at the timescales of SMBA binaries since first evolving out of the main belt and compute expected lifetimes that binaries tend to persist in NEO space until being disrupted. The caveat here however, is that most known asteroid pairs are observed in the inner main belt. While there have been a few observations of pairs in the NEO population, it is likely that their orbital parameters quickly spread from planetary encounters and chaotic evolution, making them impossible to detect unless they are newly formed (Pravec and Vokrouhlický, 2009; Pravec et al., 2019; Moskovitz et al., 2019). Ultimately, we encourage collaboration with researchers interested in using our tool for any of the ideas presented here or for topics we have not considered.

6. Conclusions

In this work, we model the dynamical survivability of near-Earth and small main belt binary asteroids to determine the source regions and lifetimes of satellites. We simulate the migration of test binaries from the ν_6 secular resonance and 3:1 mean motion resonance with Jupiter along various pre-computed pathways provided by the NEOMOD numerical integration runs. First-order analytical equations are used (i) to evaluate the changes in mutual orbit and satellite attitude for all test binaries at every planetary encounter per each migration pathway, and (ii) to propagate analytical equations in the migration segments between each planetary encounter, incorporating mutual orbit expansion and contraction induced by tidal dissipation and the BYORP effect. Successive planetary encounters and tidal-BYORP evolution arcs are modeled until the test binary reaches the observed heliocentric location of a known binary asteroid system, or the satellite either collides into or is stripped from the primary.

Using our code, we simulated the dynamical evolution and survivability of three known near-Earth systems: 1999 KW4 (with primary, Moshup and satellite, Squannit), Didymos and Dimorphos, and Bennu with a prescribed pseudo-satellite. We report survival statistics, ages, and bounding regions where satellite formation is possible in heliocentric space for each system, as well as resulting mutual orbit parameters for the two real binaries.

The main findings from this study are summarized with a bulleted list:

1. NEOs with orbits deeply within NEO space are more likely to form satellites within NEO space rather than have those satellites originate in the main belt. Our model results indicate that Didymos exhibits a significant likelihood of forming and retaining a satellite from the main belt, based on our sample-driven statistics. It remains an open question whether this dynamical trend applies to other Didymos-like systems or if the Didymos system itself possesses uniquely singular characteristics.
2. Binary inclinations may be produced by close planetary encounters.
3. Binary dynamical lifetimes can be much longer than previously suspected due to tidal-BYORP equilibrium. If this mechanism is weaker than predicted, however, our predicted model ages for our binaries will decrease.

4. It is plausible that Bennu once formed and subsequently lost a satellite due to the short-lived nature of satellites in our Bennu runs. This could explain its physical properties resembling those of a typical primary in a binary system formed through YORP spin-up-induced fission.

CRediT authorship contribution statement

Rachel H. Cueva: Writing – review & editing, Writing – original draft, Visualization, Validation, Software, Resources, Methodology, Investigation, Funding acquisition, Formal analysis, Data curation, Conceptualization. **William F. Bottke:** Writing – review & editing, Supervision, Resources, Project administration, Methodology, Funding acquisition, Conceptualization. **Jay W. McMahon:** Writing – review & editing, Supervision, Resources, Project administration, Methodology, Conceptualization. **David Nesvorný:** Writing – review & editing, Validation, Software, Resources, Methodology. **Kevin J. Walsh:** Writing – review & editing, Validation, Methodology. **David Vokrouhlický:** Writing – review & editing, Validation, Methodology. **Harrison F. Agrusa:** Writing – review & editing, Validation, Methodology.

Declaration of generative AI and AI-assisted technologies in the manuscript preparation process

During the preparation of this work the author(s) used OpenAI's ChatGPT in order to solely assist with grammar and conciseness of the writing. No technical information was generated with ChatGPT. After using this tool/service, the author(s) reviewed and edited the content as needed and take(s) full responsibility for the content of the published article.

Declaration of competing interest

The authors declare that they have no known competing financial interests or personal relationships that could have appeared to influence the work reported in this paper.

Acknowledgments

We thank Alex Meyer for useful discussions that improved the quality of this paper. R.H.C. acknowledges that this material is based upon work supported by the National Science Foundation Graduate Research Fellowship Program under Grant No. DGE 2040434. Any opinions, findings, and conclusions or recommendations expressed in this material are those of the author(s) and do not necessarily reflect the views of the National Science Foundation. Additional support for the work in the paper was provided by NASA's New Frontiers Data Analysis program through grant 80NSSC21K0828. The work of D. N. was supported by the NASA SSW program. The work of D. V. was supported by the Czech Science Foundation, Czechia (grant 25-16507S). H.F.A. thanks CNES for support.

Appendix A. Supplementary data

Supplementary material related to this article can be found online at https://doi.org/10.1016/j.icarus.2026.117048.

Data availability

Data will be made available on request.

References

Agrusa, H., Ballouz, R., Meyer, A.J., Tasev, E., Noiset, G., Karatekin, Ö., Michel, P., Richardson, D.C., Hirabayashi, M., 2022. Rotation-induced granular motion on the secondary component of binary asteroids: Application to the DART impact on dimorphos. Astron. Astrophys. 664, L3. http://dx.doi.org/10.1051/0004-6361/202244388.

Agrusa, H.F., Zhang, Y., Richardson, D.C., Pravec, P., Ćuk, M., Michel, P., Ballouz, R.L., Jacobson, S.A., Scheeres, D.J., Walsh, K., et al., 2024. Direct N-body simulations of satellite formation around small asteroids: Insights from DART's encounter with the didymos system. Planet. Sci. J. 5 (2), 54. http://dx.doi.org/10.3847/PSJ/ad206b.

Araujo, R., Winter, O., 2014. Near-earth asteroid binaries in close encounters with the earth. Astron. Astrophys. 566, A23. http://dx.doi.org/10.1051/0004-6361/201322979.

Barnouin, O., Ballouz, R.L., Marchi, S., Vincent, J.B., Agrusa, H., Zhang, Y., Ernst, C.M., Pajola, M., Tusberti, F., Lucchetti, A., et al., 2024. The geology and evolution of the near-earth binary asteroid system (65803) didymos. Nat. Commun. 15 (1), 6202. http://dx.doi.org/10.1038/s41467-024-50146-x.

Benner, L.A., Busch, M.W., Giorgini, J.D., Taylor, P.A., Margot, J.L., 2015. Radar observations of near-earth and main-belt asteroids. Asteroids IV 1, 165–182. http://dx.doi.org/10.2458/azu_uapress_9780816532131-ch009.

Bottke, W.F., Melosh, H.J., 1996. Binary asteroids and the formation of doublet craters. Icarus 124 (2), 372–391. http://dx.doi.org/10.1006/icar.1996.0215.

Bottke, W.F., Meyer, A.J., Vokrouhlický, D., Nesvorný, D., Bierhaus, E.B., DellaGiustina, D.N., Hoover, R., Connolly, H.C., Lauretta, D.S., 2025. Surface ages for the sample return asteroids bennu, ryugu, and itokawa. Planet. Sci. J. 6 (6), 150. http://dx.doi.org/10.3847/PSJ/add46a.

Bottke, W.F., Morbidelli, A., Jedicke, R., Petit, J.M., Levison, H.F., Michel, P., Metcalfe, T.S., 2002. Debiased orbital and absolute magnitude distribution of the near-earth objects. Icarus 156 (2), 399–433. http://dx.doi.org/10.1006/icar.2001.6788.

Bottke, W.F., Nolan, M.C., Greenberg, R., Kolvoord, R.A., 1994. Collisional lifetimes and impact statistics of near-earth asteroids. In: Hazards Due to Comets Asteroids, vol. 337, Univ. of Arizona Press Tucson.

Bottke, W.F., Vokrouhlický, D., Broz, M., Nesvorny, D., Morbidelli, A., 2001. Dynamical spreading of asteroid families by the Yarkovsky effect. Science 294 (5547), 1693–1696. http://dx.doi.org/10.1126/science.1066760.

Bottke, W.F., Vokrouhlický, D., Rubincam, D.P., Nesvorný, D., 2006. The Yarkovsky and YORP effects: Implications for asteroid dynamics. Annu. Rev. Earth Planet. Sci. 34 (1), 157–191. http://dx.doi.org/10.1146/annurev.earth.34.031405.125154.

Bottke, W.F., Vokrouhlický, D., Walsh, K.J., Delbo, M., Michel, P., Lauretta, D.S., Campins, H., Connolly, Jr., H.C., Scheeres, D.J., Chelsey, S.R., 2015. In search of the source of asteroid (101955) bennu: Applications of the stochastic YORP model. Icarus 247, 191–217. http://dx.doi.org/10.1016/j.icarus.2014.09.046.

Burnett, E.R., Fodde, I., Ferrari, F., 2024. Exploring tidal dissipation in rubble pile binary secondaries using a discrete element model. http://dx.doi.org/10.48550/arXiv.2410.09266, arXiv preprint arXiv:2410.09266.

Chabot, N.L., Rivkin, A.S., Cheng, A.F., Barnouin, O.S., Fahnestock, E.G., Richardson, D.C., Stickle, A.M., Thomas, C.A., Ernst, C.M., Daly, R.T., et al., 2024. Achievement of the planetary defense investigations of the double asteroid redirection test (DART) mission. Planet. Sci. J. 5 (2), 49. http://dx.doi.org/10.3847/PSJ/ad16e6.

Chauvineua, B., Farinella, P., Harris, A., 1995. The evolution of earth-approaching binary asteroids: A Monte Carlo dynamical model. Icarus 115 (1), 36–46. http://dx.doi.org/10.1006/icar.1995.1076.

Chesley, S.R., Makadia, R., Herald, D., Farnocchia, D., Chabot, N.L., Naidu, S.P., Rivkin, A.S., Siakas, A., Souami, D., Tanga, P., Tsavdaridis, S., Tsiganis, K., Bouquillon, S., Eggl, S., 2025. First detection of an asteroid's heliocentric deflection: The didymos system after DART. In: EPSC–DPS Joint Meeting 2025. Helsinki, Finland, pp. EPSC–DPS2025. http://dx.doi.org/10.5194/epsc-dps2025-1331.

Collins, B.F., Sari, R., 2008. Levy flights of binary orbits due to impulsive encounters. Astron. J. 136 (6), 2552. http://dx.doi.org/10.1088/0004-6256/136/6/2552.

Cueva, R.H., McMahon, J.W., Meyer, A.J., Scheeres, D.J., Hirabayashi, M., Raducan, S.D., Jacobson, S.A., Merrill, C.C., 2024. The secular dynamical evolution of binary asteroid system (65803) didymos post-DART. Planet. Sci. J. 5 (2), 48. http://dx.doi.org/10.3847/PSJ/ad2173.

Ćuk, M., 2007. Formation and destruction of small binary asteroids. Astrophys. J. 659 (1), L57. http://dx.doi.org/10.1086/516572.

Ćuk, M., Agrusa, H., Cueva, R.H., Ferrari, F., Hirabayashi, M., Jacobson, S.A., McMahon, J., Michel, P., Sánchez, P., Scheeres, D.J., et al., 2024. Byorp and dissipation in binary asteroids: Lessons from dart. Planet. Sci. J. 5 (7), 166. http://dx.doi.org/10.3847/PSJ/ad5d5e.

Ćuk, M., Burns, J.A., 2005. Effects of thermal radiation on the dynamics of binary NEAs. Icarus 176 (2), 418–431. http://dx.doi.org/10.1016/j.icarus.2005.02.001.

Ćuk, M., Jacobson, S.A., Walsh, K.J., 2021. Barrel instability in binary asteroids. Planet. Sci. J. 2 (6), 231. http://dx.doi.org/10.3847/PSJ/ac3093.

Ćuk, M., Nesvorný, D., 2010. Orbital evolution of small binary asteroids. Icarus 207 (2), 732–743. http://dx.doi.org/10.1016/j.icarus.2009.12.005.

Daly, R.T., Ernst, C.M., Barnouin, O.S., Chabot, N.L., Rivkin, A.S., Cheng, A.F., Adams, E.Y., Agrusa, H.F., Abel, E.D., Alford, A.L., et al., 2023. Successful kinetic impact into an asteroid for planetary defence. Nature 616 (7957), 443–447. http://dx.doi.org/10.1038/s41586-023-05810-5.

Davis, A.B., Scheeres, D.J., 2020. Doubly synchronous binary asteroid mass parameter observability. Icarus 341, 113439. http://dx.doi.org/10.1016/j.icarus.2019.113439.

Durda, D.D., Bottke, W.F., Enke, B.L., Merline, W.J., Asphaug, E., Richardson, D.C., Leinhardt, Z.M., 2004. The formation of asteroid satellites in large impacts: results from numerical simulations. Icarus 167 (2), 382–396. http://dx.doi.org/10.1016/j.icarus.2003.09.017.

Durda, D.D., Bottke, W.F., Nesvorný, D., Enke, B.L., Merline, W.J., Asphaug, E., Richardson, D.C., 2007. Size–frequency distributions of fragments from SPH/N-body simulations of asteroid impacts: Comparison with observed asteroid families. Icarus 186 (2), 498–516. http://dx.doi.org/10.1016/j.icarus.2006.09.013.

Durda, D., Enke, B., Merline, W., Richardson, D., Asphaug, E., Bottke, W., 2010. Comparing the properties of observed main-belt asteroid binaries and modeled escaping ejecta binaries (EEBs) from numerical simulations. In: 41st Annual Lunar and Planetary Science Conference. (1533), p. 2558.

Ďurech, J., Vokrouhlický, D., Pravec, P., Krugly, Y., Polishook, D., Hanuš, J., Marchis, F., Rożek, A., Snodgrass, C., Alegre, L., et al., 2024. Secular change in the spin states of asteroids due to radiation and gravitation torques-new detections and updates of the YORP effect. Astron. Astrophys. 682, A93. http://dx.doi.org/10.1051/0004-6361/202348350.

Efroimsky, M., 2015. Tidal evolution of asteroidal binaries. Ruled by viscosity. Ignorant of rigidity. Astron. J. 150 (4), 98. http://dx.doi.org/10.1088/0004-6256/150/4/98.

Fahnestock, E.G., Scheeres, D.J., 2008. Simulation and analysis of the dynamics of binary near-earth asteroid (66391) 1999 KW4. Icarus 194 (2), 410–435. http://dx.doi.org/10.1016/j.icarus.2007.11.007.

Fang, J., Margot, J.L., 2011a. Binary asteroid encounters with terrestrial planets: Timescales and effects. Astron. J. 143 (1), 25. http://dx.doi.org/10.1088/0004-6256/143/1/25.

Fang, J., Margot, J.L., 2011b. Near-earth binaries and triples: origin and evolution of spin-orbital properties. Astron. J. 143 (1), 24. http://dx.doi.org/10.1088/0004-6256/143/1/24.

Farinella, P., 1992. Evolution of earth-crossing binary asteroids due to gravitational encounters with the earth. Icarus 96 (2), 284–285. http://dx.doi.org/10.1016/0019-1035(92)90081-H.

Farinella, P., Chauvineau, B., 1993. On the evolution of binary earth-approaching asteriods. Astron. Astrophys. (ISSN: 0004-6361) 279 (1), 251–259.

Feng, S., Hu, S., Chen, X., Zhou, L., Xu, Y., Qi, Z., 2025. Evidence for YORP-induced spin deceleration in asteroid (433) eros. Astrophys. J. 986 (2), 172. http://dx.doi.org/10.3847/1538-4357/addd23.

Gladman, B., Michel, P., Froeschlé, C., 2000. The near-earth object population. Icarus 146 (1), 176–189. http://dx.doi.org/10.1006/icar.2000.6391.

Goldreich, P., Sari, R., 2009. Tidal evolution of rubble piles. Astrophys. J. 691 (1), 54. http://dx.doi.org/10.1088/0004-637X/691/1/54.

Golubov, O., 2017. Analytic model for tangential YORP. Astron. J. 154 (6), 238. http://dx.doi.org/10.3847/1538-3881/aa88ba.

Golubov, O., Krugly, Y.N., 2012. Tangential component of the YORP effect. Astrophys. J. Lett. 752 (1), L11. http://dx.doi.org/10.1088/2041-8205/752/1/L11.

Granvik, M., Morbidelli, A., Jedicke, R., Bolin, B., Bottke, W.F., Beshore, E., Vokrouhlický, D., Delbó, M., Michel, P., 2016. Super-catastrophic disruption of asteroids at small perihelion distances. Nature 530 (7590), 303–306. http://dx.doi.org/10.1038/nature16934.

Heggie, D.C., Rasio, F.A., 1996. The effect of encounters on the eccentricity of binaries in clusters. Mon. Not. R. Astron. Soc. 282 (3), 1064–1084. http://dx.doi.org/10.1093/mnras/282.3.1064.

Herrera, C., Carry, B., Lagain, A., Vavilov, D.E., 2024. Binary craters on ceres and vesta and implications for binary asteroids. Astron. Astrophys. 688, A176. http://dx.doi.org/10.1051/0004-6361/202449502.

Jacobson, S.A., Marzari, F., Rossi, A., Scheeres, D.J., 2016. Matching asteroid population characteristics with a model constructed from the YORP-induced rotational fission hypothesis. Icarus 277, 381–394. http://dx.doi.org/10.1016/j.icarus.2016.05.032.

Jacobson, S.A., Scheeres, D.J., 2011a. Dynamics of rotationally fissioned asteroids: Source of observed small asteroid systems. Icarus 214 (1), 161–178. http://dx.doi.org/10.1016/j.icarus.2011.04.009.

Jacobson, S.A., Scheeres, D.J., 2011b. Long-term stable equilibria for synchronous binary asteroids. Astrophys. J. Lett. 736 (1), L19. http://dx.doi.org/10.1088/2041-8205/736/1/L19.

Jacobson, S.A., Scheeres, D.J., McMahon, J., 2013. Formation of the wide asynchronous binary asteroid population. Astrophys. J. 780 (1), 60. http://dx.doi.org/10.1088/0004-637X/780/1/60.

Kawaguchi, J., Fujiwara, A., Uesugi, T., 2008. Hayabusa—Its technology and science accomplishment summary and hayabusa-2. Acta Astronaut. 62 (10–11), 639–647. http://dx.doi.org/10.1016/j.actaastro.2008.01.028.

Lauretta, D., Balram-Knutson, S., Beshore, E., Boynton, W., Drouet d'Aubigny, C., DellaGiustina, D., Enos, H., Golish, D., Hergenrother, C., Howell, E., et al., 2017. OSIRIS-REx: sample return from asteroid (101955) bennu. Space Sci. Rev. 212 (1), 925–984. http://dx.doi.org/10.1007/s11214-017-0405-1.

Lauretta, D.S., Connolly, Jr., H.C., Aebersold, J.E., Alexander, C.M.O., Ballouz, R.L., Barnes, J.J., Bates, H.C., Bennett, C.A., Blanche, L., Blumenfeld, E.H., et al., 2024. Asteroid (101955) bennu in the laboratory: Properties of the sample collected by OSIRIS-REx. Meteorit. Planet. Sci. 59 (9), 2453–2486. http://dx.doi.org/10.1111/maps.14227.

Lauretta, D., DellaGiustina, D., Bennett, C., Golish, D., Becker, K., Balram-Knutson, S., Barnouin, O., Becker, T., Bottke, W., Boynton, W., et al., 2019. The unexpected surface of asteroid (101955) bennu. Nature 568 (7750), 55–60. http://dx.doi.org/10.1038/s41586-019-1033-6.

Levison, H.F., Marchi, S., Noll, K.S., Spencer, J.R., Statler, T.S., Bell, III, J.F., Bierhaus, E.B., Binzel, R., Bottke, W.F., Britt, D., et al., 2024. A contact binary satellite of the asteroid (152830) Dinkinesh. Nature 629 (8014), 1015–1020. http://dx.doi.org/10.1038/s41586-024-07378-0.

Lucchetti, A., Cambioni, S., Nakano, R., Barnouin, O., Pajola, M., Penasa, L., Tusberti, F., Ramesh, K., Dotto, E., Ernst, C., et al., 2024. Fast boulder fracturing by thermal fatigue detected on stony asteroids. Nat. Commun. 15 (1), 6206. http://dx.doi.org/10.1038/s41467-024-50145-y.

Margot, J.L., Nolan, M., Benner, L., Ostro, S., Jurgens, R., Giorgini, J., Slade, M., Campbell, D., 2002. Binary asteroids in the near-earth object population. Science 296 (5572), 1445–1448. http://dx.doi.org/10.1126/science.1072094.

Margot, J.L., Pravec, P., Taylor, P., Carry, B., Jacobson, S., 2015. Asteroid systems: binaries, triples, and pairs. Asteroids IV 355, 373. http://dx.doi.org/10.2458/azu_uapress_9780816532131-ch019.

McMahon, J., Scheeres, D., 2010a. Detailed prediction for the BYORP effect on binary near-earth asteroid (66391) 1999 KW4 and implications for the binary population. Icarus 209 (2), 494–509. http://dx.doi.org/10.1016/j.icarus.2010.05.016.

McMahon, J., Scheeres, D., 2010b. Secular orbit variation due to solar radiation effects: a detailed model for BYORP. Celest. Mech. Dyn. Astron. 106 (3), 261–300. http://dx.doi.org/10.1007/s10569-009-9247-9.

Meyer, A.J., Agrusa, H.F., Richardson, D.C., Daly, R.T., Fuentes-Muñoz, O., Hirabayashi, M., Michel, P., Merrill, C.C., Nakano, R., Cheng, A.F., et al., 2023a. The perturbed full two-body problem: application to post-DART didymos. Planet. Sci. J. 4 (8), 141. http://dx.doi.org/10.3847/PSJ/acebc7.

Meyer, A.J., Fuentes-Muñoz, O., Gkolias, I., Tsiganis, K., Pravec, P., Naidu, S., Scheeres, D.J., 2024. An earth encounter as the cause of chaotic dynamics in binary asteroid (35107) 1991vh. Planet. Sci. J. 5 (8), 179. http://dx.doi.org/10.3847/PSJ/ad6605.

Meyer, A.J., Scheeres, D.J., 2021. The effect of planetary flybys on singly synchronous binary asteroids. Icarus 367, 114554. http://dx.doi.org/10.1016/j.icarus.2021.114554.

Meyer, A.J., Scheeres, D.J., Agrusa, H.F., Noiset, G., McMahon, J., Karatekin, Ö., Hirabayashi, M., Nakano, R., 2023b. Energy dissipation in synchronous binary asteroids. Icarus 391, 115323. http://dx.doi.org/10.1016/j.icarus.2022.115323.

Michel, P., Zappalá, V., Cellino, A., Tanga, P., 2000. Estimated abundance of atens and asteroids evolving on orbits between earth and sun. Icarus 143 (2), 421–424. http://dx.doi.org/10.1006/icar.1999.6282.

Minker, K., Carry, B., Vachier, F., Scheirich, P., Pravec, P., Müller, T., Moór, A., Arcidiacono, C., Conrad, A., Veillet, C., et al., 2025. Orbits of very distant asteroid satellites. Astron. Astrophys. 698, A136. http://dx.doi.org/10.1051/0004-6361/202451124.

Minton, D.A., Malhotra, R., 2010. Dynamical erosion of the asteroid belt and implications for large impacts in the inner solar system. Icarus 207 (2), 744–757. http://dx.doi.org/10.1016/j.icarus.2009.12.008.

Morbidelli, A., Vokrouhlický, D., 2003. The Yarkovsky-driven origin of near-earth asteroids. Icarus 163 (1), 120–134. http://dx.doi.org/10.1016/S0019-1035(03)00047-2.

Moskovitz, N.A., Fatka, P., Farnocchia, D., Devogéle, M., Polishook, D., Thomas, C.A., Mommert, M., Avner, L.D., Binzel, R.P., Burt, B., et al., 2019. A common origin for dynamically associated near-earth asteroid pairs. Icarus 333, 165–176. http://dx.doi.org/10.1016/j.icarus.2019.05.030.

Murray, C.D., Dermott, S.F., 1999. Solar System Dynamics. Cambridge University Press.

Naidu, S.P., Margot, J.L., Taylor, P.A., Nolan, M.C., Busch, M.W., Benner, L.A., Brozovic, M., Giorgini, J.D., Jao, J.S., Magri, C., 2015. Radar imaging and characterization of the binary near-earth asteroid (185851) 2000 DP107. Astron. J. 150 (2), 54. http://dx.doi.org/10.1088/0004-6256/150/2/54.

Nesvorný, D., Deienno, R., Bottke, W.F., Jedicke, R., Naidu, S., Chesley, S.R., Chodas, P.W., Granvik, M., Vokrouhlický, D., Brož, M., et al., 2023. NEOMOD: a new orbital distribution model for near-earth objects. Astron. J. 166 (2), 55. http://dx.doi.org/10.3847/1538-3881/ace040.

Nesvorný, D., Enke, B.L., Bottke, W.F., Durda, D.D., Asphaug, E., Richardson, D.C., 2006. Karin cluster formation by asteroid impact. Icarus 183 (2), 296–311. http://dx.doi.org/10.1016/j.icarus.2006.03.008.

Nesvorný, D., Vokrouhlický, D., Shelly, F., Deienno, R., Bottke, W.F., Christensen, E., Jedicke, R., Naidu, S., Chesley, S.R., Chodas, P.W., et al., 2024a. NEOMOD 2: An updated model of near-earth objects from a decade of catalina sky survey observations. Icarus 411, 115922. http://dx.doi.org/10.1016/j.icarus.2023.115922.

Nesvorný, D., Vokrouhlický, D., Shelly, F., Deienno, R., Bottke, W.F., Fuls, C., Jedicke, R., Naidu, S., Chesley, S.R., Chodas, P.W., et al., 2024b. NEOMOD 3: The debiased size distribution of near earth objects. Icarus 417, 116110. http://dx.doi.org/10.1016/j.icarus.2024.116110.

Nimmo, F., Matsuyama, I., 2019. Tidal dissipation in rubble-pile asteroids. Icarus 321, 715–721. http://dx.doi.org/10.1016/j.icarus.2018.12.012.

Ostro, S.J., Margot, J.L., Benner, L.A., Giorgini, J.D., Scheeres, D.J., Fahnestock, E.G., Broschart, S.B., Bellerose, J., Nolan, M.C., Magri, C., et al., 2006. Radar imaging of binary near-earth asteroid (66391) 1999 KW4. Science 314 (5803), 1276–1280. http://dx.doi.org/10.1126/science.1133622.

Polishook, D., Brosch, N., Prialnik, D., 2011. Rotation periods of binary asteroids with large separations–confronting the escaping ejecta binaries model with observations. Icarus 212 (1), 167–174. http://dx.doi.org/10.1016/j.icarus.2010.12.020.

Pou, L., Nimmo, F., 2024. Tidal dissipation of binaries in asteroid pairs. Icarus 411, 115919. http://dx.doi.org/10.1016/j.icarus.2023.115919.

Pravec, P., 2025. Physical parameters of near-earth and small main-belt binary asteroids. Bin. Sol. Syst. VI.

Pravec, P., Fatka, P., Vokrouhlický, D., Scheirich, P., Ďurech, J., Scheeres, D., Kušnirak, P., Hornoch, K., Galad, A., Pray, D., et al., 2019. Asteroid pairs: a complex picture. Icarus 333, 429–463. http://dx.doi.org/10.1016/j.icarus.2019.05.014.

Pravec, P., Harris, A.W., 2007. Binary asteroid population: 1. Angular momentum content. Icarus 190 (1), 250–259. http://dx.doi.org/10.1016/j.icarus.2007.02.023.

Pravec, P., Scheirich, P., 2012. Small binary asteroids and prospects for their observations with gaia. Planet. Space Sci. 73 (1), 56–61. http://dx.doi.org/10.1016/j.pss.2012.04.006.

Pravec, P., Scheirich, P., Kušnirák, P., Hornoch, K., Galád, A., Naidu, S., Pray, D., Világi, J., Gajdoš, v., Kornoš, L., et al., 2016. Binary asteroid population. 3. Secondary rotations and elongations. Icarus 267, 267–295. http://dx.doi.org/10.1016/j.icarus.2015.12.019.

Pravec, P., Scheirich, P., Kušnirák, P., Šarounová, L., Mottola, S., Hahn, G., Brown, P., Esquerdo, G., Kaiser, N., Krzeminski, Z., et al., 2006. Photometric survey of binary near-earth asteroids. Icarus 181 (1), 63–93. http://dx.doi.org/10.1016/j.icarus.2005.10.014.

Pravec, P., Scheirich, P., Vokrouhlický, D., Harris, A., Kušnirák, P., Hornoch, K., Pray, D., Higgins, D., Galád, A., Világi, J., et al., 2012. Binary asteroid population. 2. Anisotropic distribution of orbit poles of small, inner main-belt binaries. Icarus 218 (1), 125–143. http://dx.doi.org/10.1016/j.icarus.2011.11.026.

Pravec, P., Vokrouhlický, D., 2009. Significance analysis of asteroid pairs. Icarus 204 (2), 580–588. http://dx.doi.org/10.1016/j.icarus.2009.07.004.

Pravec, P., Vokrouhlický, D., Polishook, D., Scheeres, D.J., Harris, A.W., Galad, A., Vaduvescu, O., Pozo, F., Barr, A., Longa, P., et al., 2010. Formation of asteroid pairs by rotational fission. Nature 466 (7310), 1085–1088. http://dx.doi.org/10.1038/nature09315.

Pravec, P., Wolf, M., Šarounová, L., 1998. Occultation/eclipse events in binary asteroid 1991 VH. Icarus 133 (1), 79–88. http://dx.doi.org/10.1006/icar.1998.5890.

Raducan, S., Madeira, G., Agrusa, H., Merrill, C., Marschall, R., Ferrari, F., Wimarsson, J., Charnoz, S., Michel, P., Jutzi, M., 2025. Multiple moonlet mergers as the origin of the Dinkinesh-Selam system. Nat. Commun. 16 (1), 11033, doi:Multiple moonlet mergers as the origin of the Dinkinesh-Selam system.

Richardson, D.C., Agrusa, H.F., Barbee, B., Bottke, W.F., Cheng, A.F., Eggl, S., Ferrari, F., Hirabayashi, M., Karatekin, Ö., McMahon, J., et al., 2022. Predictions for the dynamical states of the didymos system before and after the planned DART impact. Planet. Sci. J. 3 (7), 157. http://dx.doi.org/10.3847/PSJ/ac76c9.

Richardson, D.C., Agrusa, H.F., Barbee, B., Cueva, R.H., Ferrari, F., Jacobson, S.A., Makadia, R., Meyer, A.J., Michel, P., Nakano, R., et al., 2024. The dynamical state of the didymos system before and after the DART impact. Planet. Sci. J. 5 (8), 182. http://dx.doi.org/10.3847/PSJ/ad62f5.

Richardson, D.C., Barnouin, O.S., Benner, L.A., Bottke, W., Bagatin, A.C., Cheng, A.F., Eggl, S., Hamilton, D.P., Hestroffer, D., Hirabayashi, M., et al., 2016. Dynamical and physical properties of 65803 didymos, the proposed aida mission target. In: AAS/Division for Planetary Sciences Meeting# 48, vol. 48, 123-117.

Richardson, J.E., Steckloff, J.K., Minton, D.A., 2020. Impact-produced seismic shaking and regolith growth on asteroids 433 Eros, 2867 Šteins, and 25143 Itokawa. Icarus 347, 113811. http://dx.doi.org/10.1016/j.icarus.2020.113811.

Rubincam, D.P., 2000. Radiative spin-up and spin-down of small asteroids. Icarus 148 (1), 2–11. http://dx.doi.org/10.1006/icar.2000.6485.

Scheeres, D.J., 2006. Relative equilibria for general gravity fields in the sphere-restricted full 2-body problem. Celest. Mech. Dyn. Astron. 94 (3), 317–349. http://dx.doi.org/10.1007/s10569-005-6182-2.

Scheeres, D.J., 2007a. The dynamical evolution of uniformly rotating asteroids subject to YORP. Icarus 188 (2), 430–450. http://dx.doi.org/10.1016/j.icarus.2006.12.015.

Scheeres, D.J., 2007b. Rotational fission of contact binary asteroids. Icarus 189 (2), 370–385. http://dx.doi.org/10.1016/j.icarus.2007.02.015.

Scheeres, D.J., 2015. Landslides and mass shedding on spinning spheroidal asteroids. Icarus 247, 1–17. http://dx.doi.org/10.1016/j.icarus.2014.09.017.

Scheeres, D.J., Fahnestock, E.G., Ostro, S.J., Margot, J.L., Benner, L.A., Broschart, S.B., Bellerose, J., Giorgini, J.D., Nolan, M.C., Magri, C., et al., 2006. Dynamical configuration of binary near-earth asteroid (66391) 1999 KW4. Science 314 (5803), 1280–1283. http://dx.doi.org/10.1126/science.1133599.

Scheeres, D., McMahon, J., French, A., Brack, D., Chesley, S., Farnocchia, D., Takahashi, Y., Leonard, J., Geeraert, J., Page, B., et al., 2019. The dynamic geophysical environment of (101955) bennu based on OSIRIS-REx measurements. Nat. Astron. 3 (4), 352–361. http://dx.doi.org/10.1038/s41550-019-0721-3.

Scheirich, P., Pravec, P., 2009. Modeling of lightcurves of binary asteroids. Icarus 200 (2), 531–547. http://dx.doi.org/10.1016/j.icarus.2008.12.001.

Scheirich, P., Pravec, P., Jacobson, S., Ďurech, J., Kušnirák, P., Hornoch, K., Mottola, S., Mommert, M., Hellmich, S., Pray, D., et al., 2015. The binary near-earth asteroid (175706) 1996 FG3—An observational constraint on its orbital evolution. Icarus 245, 56–63. http://dx.doi.org/10.1016/j.icarus.2014.09.023.

Stern, S.A., 2009. Ejecta exchange and satellite color evolution in the pluto system, with implications for KBOs and asteroids with satellites. Icarus 199 (2), 571–573. http://dx.doi.org/10.1016/j.icarus.2008.10.006.

Taylor, P.A., Margot, J.L., 2011. Binary asteroid systems: Tidal end states and estimates of material properties. Icarus 212 (2), 661–676. http://dx.doi.org/10.1016/j.icarus.2011.01.030.

Vavilov, D.E., Carry, B., Lagain, A., Guimpier, A., Conway, S., Devillepoix, H., Bouley, S., 2022. Evidence for widely-separated binary asteroids recorded by craters on mars. Icarus 383, 115045. http://dx.doi.org/10.1016/j.icarus.2022.115045.

Vincent, J.B., Asphaug, E., Barnouin, O., Beccarelli, J., Benavidez, P.G., Campo-Bagatin, A., Chabot, N.L., Ernst, C.M., Hasselmann, P.H., Hirabayashi, M., et al., 2024. Macroscale roughness reveals the complex history of asteroids didymos and dimorphos. Planet. Sci. J. 5 (10), 236. http://dx.doi.org/10.3847/PSJ/ad7a01.

Virkki, A.K., Marshall, S.E., Venditti, F.C., Zambrano-Marín, L.F., Hickson, D.C., McGilvray, A., Taylor, P.A., Rivera-Valentín, E.G., Devogéle, M., Díaz, E.F., et al., 2022. Arecibo planetary radar observations of near-earth asteroids: 2017 december–2019 december. Planet. Sci. J. 3 (9), 222. http://dx.doi.org/10.3847/PSJ/ac8b72.

Vokrouhlický, D., Bottke, W.F., Chesley, S.R., Scheeres, D.J., Statler, T.S., 2015. The Yarkovsky and YORP Effects. In: Michel, P., DeMeo, F.E., Bottke, W.F. (Eds.), Asteroids IV. pp. 509–531. http://dx.doi.org/10.2458/azu_uapress_9780816532131-ch027.

Vokrouhlický, D., Nesvorný, D., 2008. Pairs of asteroids probably of a common origin. Astron. J. 136 (1), 280–290. http://dx.doi.org/10.1088/0004-6256/136/1/280.

Vokrouhlický, D., Nesvorný, D., Brož, M., Bottke, W.F., 2024. Debiased population of very young asteroid families. Astron. Astrophys. 681, A23. http://dx.doi.org/10.1051/0004-6361/202347670.

Vokrouhlický, D., Čapek, D., Chesley, S., Ostro, S., 2005. Yarkovsky detection opportunities: II. binary systems. Icarus 179 (1), 128–138. http://dx.doi.org/10.1016/j.icarus.2005.06.003.

Walsh, K.J., 2018. Rubble pile asteroids. Annu. Rev. Astron. Astrophys. 56 (1), 593–624. http://dx.doi.org/10.1146/annurev-astro-081817-052013.

Walsh, K.J., Richardson, D.C., 2006. Binary near-earth asteroid formation: Rubble pile model of tidal disruptions. Icarus 180 (1), 201–216. http://dx.doi.org/10.1016/j.icarus.2005.08.015.

Walsh, K.J., Richardson, D.C., 2008. A steady-state model of NEA binaries formed by tidal disruption of gravitational aggregates. Icarus 193 (2), 553–566. http://dx.doi.org/10.1016/j.icarus.2007.08.020.

Walsh, K.J., Richardson, D.C., Michel, P., 2008. Rotational breakup as the origin of small binary asteroids. Nature 454 (7201), 188–191. http://dx.doi.org/10.1038/nature07078.

Wang, H.S., Hou, X.Y., 2021. Break-up of the synchronous state of binary asteroid systems. Mon. Not. R. Astron. Soc. 505 (4), 6037–6050. http://dx.doi.org/10.1093/mnras/stab1585.

Watanabe, S.i., Tsuda, Y., Yoshikawa, M., Tanaka, S., Saiki, T., Nakazawa, S., 2017. Hayabusa2 mission overview. Space Sci. Rev. 208 (1), 3–16. http://dx.doi.org/10.1007/s11214-017-0377-1.

Weidenschilling, S.J., Paolicchi, P., Źappala, V., 1989. Do asteroids have satellites? Asteroids II 643–658.

Zhou, W.H., 2024. The binary Yarkovsky effect on the primary asteroid with applications to singly synchronous binary asteroids. Astron. Astrophys. 692, L2. http://dx.doi.org/10.1051/0004-6361/202452146.

Zhou, W.H., Vokrouhlický, D., Kanamaru, M., Agrusa, H., Pravec, P., Delbo, M., Michel, P., 2024. The Yarkovsky effect on the long-term evolution of binary asteroids. Astrophys. J. Lett. 968 (1), L3. http://dx.doi.org/10.3847/2041-8213/ad4f7f.